

Ecofriendly Synthesis of Zinc oxide Nanoparticles by
Telosma cordata leaves

M. V. Ancy
21PCH003

Thesis submitted to
Avinashilingam Institute for Home Science and Higher Education for
Women, Coimbatore-641 043

In Partial Fulfillment of the Requirements for the Degree of
Master of Science in Chemistry


May - 2023

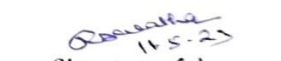
Eco-friendly Synthesis of Zinc oxide nanoparticles by
Telosma cordata leaves

ANCY M V
21PCH013

Thesis submitted to
Avinashilingam Institute for Home Science and Higher Education for Women
Coimbatore- 641 043

In Partial Fulfilment of the Requirements for the Degree of
Master of Science in Chemistry
May - 2023


Signature of the
Supervisor


Signature of the
Head of the Department

ACKNOWLEDGEMENT

ACKNOWLEDGEMENT

First and foremost, I thank **LORD ALMIGHTY** for his blessings and giving me the strength to carry out my research work successfully.

I take enormous pleasure in thanking **Dr. S.P. THYAGARAJAN**, Chancellor Avinashilingam Institute for Home Science and Higher Education for Women, Coimbatore, for providing the favourable infrastructure to do my research work.

I would like to thank **Dr. V. BHARATHI HARISHANKAR**, Vice Chancellor, Avinashilingam Institute for Home Science and Higher Education for Women, Coimbatore, for the encouragement and for providing the opportunity to develop and establish my skills.

I extend my thanks to **Dr. S. KOWSALYA**, Registrar, Avinashilingam Institute for Home Science and Higher Education for Women, Coimbatore, for the encouragement given by her during the investigation.

I express my heartfelt thanks to **Dr. G. PADMAVATHI**, Professor, Dean, School of Physical and Computational Sciences, Avinashilingam Institute for Home Science and Higher Education for Women, Coimbatore, for her excellent support, unflinching encouragement and guidance during the course of the investigation.

I record my deep sense of gratitude to **Dr. (Mrs) R. SARATHA, Professor and Head of the Department**, Department of Chemistry, Avinashilingam Institute for Home Science and Higher Education for Women, Coimbatore, for her constant support and tremendous care rendered for carrying out of my thesis successfully.

I extend my deep sense of gratitude to my guide **Dr. (Mrs) A. PRITHIBA, M.Sc., M.Phil., Ph.D. Assistant Professor (SS)**, Avinashilingam Institute for Home Science and Higher Education for Women, University Coimbatore for her guidance, encouragement and excellent support for the successful completion of the study.

I would like to express my sincere thanks to all the **STAFF MEMBERS OF THE DEPARTMENT OF CHEMISTRY**, Avinashilingam Institute for Home Science and Higher Education for Women, University Coimbatore, for their help and support in the successful completion of this dissertation.

My special thanks to my seniors **S.THARANI, C.DHIVYA** for their presents ,advice and support whenever needed during my studies.

My special thanks to my **BELOVED PARENTS, BROTHER** and **SISTER** for their help whenever required to complete this work.

I also thank **ALL MY FRIENDS** for their continuous encouragement and support throughout the work.

M.V.ANCY

CONTENT

S. No	List	Page No
	List of Figures	Vii
	List of Tables	Viii
	List of Abbreviations	ix
1	Introduction	2
2	Review of literature	9
3	Materials &Methods	40
4	Results & Discussion	48
5	Summary & Conclusion	67
6	Bibliography	69

LIST OF FIGURES

S.No.	Figure No.	Title	Page No.
1	1.1	Zinc oxide nanoparticles synthesized by using different source	5
2	4.1.1	Phytochemical screening	49
3	4.1.2	Biosynthesis of ZnO nanoparticles using plant extract	51
4	4.2.1	UV-Visible is spectrum of green synthesized ZnO NPs	52
5	4.2.2	Band gap energy of green synthesized ZnO NPs	53
6	4.3.1	FT-IR spectrum of green synthesized ZnO NPs	54
7	4.4.1	XRD image of green synthesized ZnO NPs	55
8	4.5.1	SEM image of green synthesized ZnO NPs	57
9	4.6.1	EDX image of green synthesized ZnO NPs	58
10	4.7.1	Antibacterial activity of Inhibition zone of green synthesized ZnO NPs	59
11	4.8.1	TGA image of green synthesized ZnO NPs	61
12	4.8.2	Derivative TG curve of green synthesized ZnO NPs	62
13	4.9.1	3-D Optical Profilometer image of green synthesized ZnO NPs	63
14	4.9.2	Histogram image of green synthesized of ZnO NPs	64
15	4.9.3	3-D Optical Profilometer of cross section	64
16	4.9.4	3-D Optical Profilometer of roughness	65

LIST OF TABLES

S.No.	TABLE.NO	TITLE	PAGE.NO
1	4.1.1	Phytochemical constituents of <i>Telosma cordata</i> leaf extract	48
2	4.3.1	Spectral range and functional group of green synthesized ZnO NPs	54
3	4.4.1	Structure and geometric parameters of green synthesized ZnO NPs	56
4	4.6.1	EDX value of green synthesized ZnO NPs	59
5	4.7.1	Zone of Inhibition	60
6	4.9.5	Ra and Rq value of green synthesized ZnO NPs	65

LIST OF ABBREVIATIONS

UV	Ultra Violet Spectroscopy
FT- IR	Fourier Transform Infrared Spectroscopy
XRD	X-Ray Diffraction
UV	Scanning Electron Microscopy
EDX	Energy Dispersive X-ray spectroscopy
TGA	Thermo gravimetric analysis

INTRODUCTION

INTRODUCTION

Nanotechnology deals with the production and usage of material with nanoscale dimension. Nanoscale dimension provides nanoparticles a large surface area to volume ratio and thus very specific properties. Nanoparticles are used immensely due to its small size, orientation, physical properties, which are reportedly shown to change the performance of any other material which is in contact with these tiny particles. Most of the new physical and chemical methods employed for the synthesis of metal oxide nanoparticles use organic solvents and toxic reducing and chelating agents, thereby threatening the environment and limiting nanoparticles applications in biomedical, biotechnological, environmental, biological, and some industrial areas. Thus, the use of suitable and biocompatible processes for the preparation of metal oxide nanoparticles has received significant attention. These processes are classified in green chemistry.

Using plant extracts in the green synthesis of nanoparticles is one of the cleanest, biocompatible, nontoxic and eco-friendly methods used for large-scale production. Literature review revealed that few studies have reported on the synthesis of some metal and metal oxide nanoparticles such as silver, ferric, copper oxide, zinc oxide, gold, copper, palladium etc.

Among the metal Oxide nanoparticles, the zinc oxide is interesting because ZnO is an inorganic compound which occurs rarely in nature and when purified, ZnO appears as white crystalline powder which is nearly insoluble in water. The semiconductor ZnO has gained substantial interest in the research community in part because of its large exciton binding energy 60 meV which could lead to lasing action based on exciton recombination even above room temperature. Due to their low toxicity and size dependent properties, ZnO nanoparticles have been widely used for various applications in textiles, cosmetics, diagnostics and even in micro-

electronics. ZnO has been found to be potentially useful and efficient than other metals for biosynthesis of nanoparticles for clinical purposes.

ZnO NPs have drawn attention of many researchers for their unique optical and chemical behaviors which can be easily tuned by changing the morphology. Within the large family of metal oxide NPs ZnO NPs have been used in various cutting edge applications like electronics, communication, sensors, cosmetics, environmental protection, biology and the medicinal industry. Moreover, ZnO NP has a tremendous potential in biological applications like biological sensing, biological labeling, gene delivery, drug delivery and nano-medicine along with its antibacterial, antifungal, acaricidal, pediculocidal, larvicidal and anti-diabetic activities

Due to its low cost, ability to be produced in ambient air, lack of toxicity, and compatibility with the environment, the synthesis of NPs using environmentally benign methods has recently gained popularity among academics. and simplicity of use as the end products are highly water soluble, biocompatible, and free of toxic stabilisers. Plant extracts have great promise for the quick and environmentally friendly production of NPs. Different researchers have used fruit juice, leaf extracts, and Aloe sp. extracts in the synthesis of ZnO NP. It has also been observed that belongs to the Malvaceae family and is generally known as Indian sorrel, in vivo synthesis of ZnO NP. In India, Africa, and Mexico, it is frequently planted for fibre and edible uses as well as traditional medicine. It was discovered that the plant's leaf and calyx extracts were diuretic, cholerectic, hypotensive, blood pressure suppressive, chemo-protective, antioxidant, anti-tumor, and anti-cancerous agents. Additionally, it has been claimed that *H. sabdariffa* is a potent antimicrobial agent and beneficial for diabetes mellitus.

In our research, we have created ZnO NP by environmentally friendly methods employing leaf extract, placing particular emphasis on the growth of NP at various temperatures. Nanostructures made of zinc oxide (ZnO) are at the forefront of study

because of their special characteristics and diverse range of uses. Due to its exceptional optical and electrical characteristics, it has a wide range of technological uses, including thin-film transistors, gas sensors, transparent conductors, biomedical, and piezoelectric applications. In the creation of solar cells, including quantum dot-sensitive solar cells, ZnO is widely used. Everyone is aware that With a relatively wide band gap (3.2-3.37 eV) and high transparency at ambient temperature, ZnO is one of the most significant semiconductor materials. Additionally, because of the substantial 60 meV exciton binding energy, it may find use in solar cells and other optoelectronic devices. Because of its environmental friendliness, stability, and ease of synthesis into various forms and sizes, it is anticipated to serve as an alternate material for TiO₂. ZnO thin films can be created using a variety of methods, including chemical vapour deposition and sputtering.

The need to create ecologically friendly synthesis processes that don't involve harmful materials is becoming more and more pressing in recent years. To date, a wide range of physical, chemical, and biological techniques have been used to create various kinds of nanoparticles. The creation of nanoparticles using various plant components is a very novel process that promotes true green chemistry by eliminating the need for harmful chemicals, high temperatures, pressures, and energies while also being highly efficient and cost-effective. Recent studies have shown that synthesising ZnO nanoparticles from environmentally safe benign materials, such as leaf extract bacterium and fungus, has several advantages in terms of compatibility with pharmaceutical and other biological applications.

In this work, we have methodically investigated the mass-level production of ZnONPs utilising tomato extract, both thermally and under various powers of microwave irradiation. Thin films of nanocomposite ZnONPs with GO and TiO₂ nanoparticles were created, and the current-voltage measurements of these nanocomposites were examined for their potential use in solar cells.

The various routes that have been used for the synthesis of ZnO nanoparticles include sol–gel synthesis, hydrothermal, solvothermal methods, microemulsion methods and precipitation method. These methods are associated with environmental contamination, high temperatures, high pressures and expensive equipment. Biological methods specifically the use of plants are becoming the most preferred methods as they are clean, cost effective, considerable rapid and often single step protocols. In addition, nanoparticles prepared using plant extract as the reducing as well as the capping agents have been found to be nontoxic and can be employed in medicine. Biosynthetic routes provide nanoparticles of better defined sizes and morphology as compared to other physicochemical methods of producing nanoparticles. Plant biomolecules are known to mediate the reduction of ions to nanoparticles and in the stabilization of the same nanoparticles.

Several studies have demonstrated the synthesis of ZnO NPs using different plant extracts. The exact physical and chemical properties of zinc oxide nanoparticles depend on the different ways they are synthesized and the plant type or source species from which plant extract is used for NPs synthesis. Due to the increasing popularity of green methods, different works have been done to synthesize ZnO NPs using different sources like bacteria, fungus, algae, plants and others (Fig. 1) .

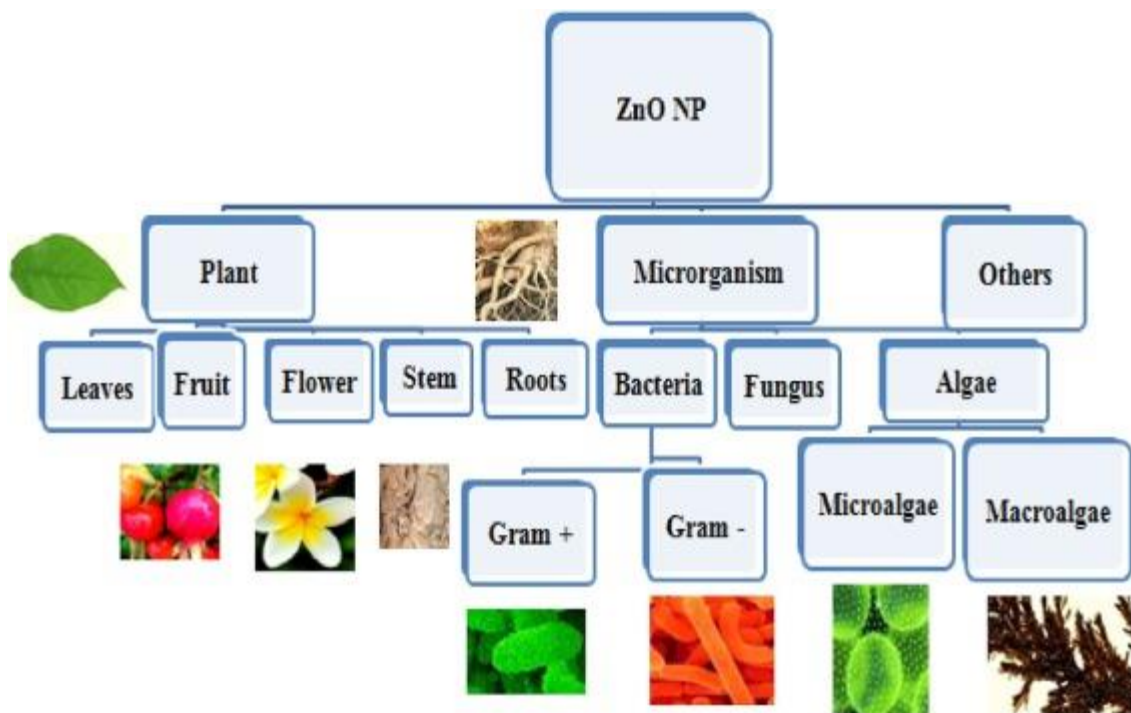


Fig. 1. Zinc oxide nanoparticle synthesis by using different sources.

Green synthesis of ZnO NPs using plant extract:

Plant parts like leaf, stem, root, fruit, and seed have been used for ZnO NPs synthesis because of the exclusive phytochemicals that they produce. Using natural extracts of plant parts is a very eco-friendly, cheap process and it does not involve usage of any intermediate base groups. It takes very less time, does not involve usage of costly equipment and precursors and gives a highly pure and quantity enriched product free of impurities. Plants are the most preferred source of NPs synthesis because they lead to large-scale production and production of stable, varied in shape and size NPs.

Most commonly applied method for simple preparation of ZnO NPs from leaves or flowers is where the plant part is washed thoroughly in running tap water and sterilized using double distilled water. Then, the plant part is kept for drying at room temperature followed by weighing and then crushing it using a mortar and

pestle. Pure distilled H₂O is added to the plant part according to the desired concentration and the mixture is boiled under continuous stirring using a magnetic stirrer. The solution is filtered using Whatman filter paper and the obtained clear solution was used as a plant extract (sample). Some volume of the extract is mixed with hydrated Zinc nitrate or zinc oxide or zinc sulfate and the mixture is boiled at desired temperature and time to achieve efficient mixing.

Some perform optimization at this point using different temperature, pH, extract concentration and time. Incubation period results in a change of color of the mixture to yellow which is a visual confirmation of the synthesized NPs. Then a UV-Vis spectrophotometry is employed to confirm the synthesis of NPs followed by centrifugation of mixture and drying the pellet in a hot air oven to get the crystal NPs. Further, synthesized nanoparticles are further characterized using X-ray diffractometer (XRD), Energy Dispersion Analysis of X-ray (EDAX), Fourier Transform Infrared Spectroscopy (FTIR), Field Emission Scanning Electron Microscopy (FE-SEM), Thermal-gravimetric Differential Thermal Analysis (TG-DTA), Raman Spectroscopy etc.

1.1 OBJECTIVES

1. To bio-synthesize ZnO nanoparticles
2. To use less chemicals and reduce waste generation
3. To characterize the synthesized ZnO nanoparticles using UV-Visible spectroscopy, FT-IR, XRD, SEM, EDAX, 3-D profilometer and perform antibacterial studies

REVIEW
OF
LITERATURE

REVIEW OF LITERATURE:

1. **Fatemeh Davar *et.al.*, (2015)** prepared a novel ZnO photocatalyst by a green method using lemon juice and zinc acetate as precursors, and then the effect of sucrose addition on the initial precursors was investigated. The samples were characterized by field emission scanning electron microscopy, X-ray diffraction, Fourier transform infrared, UV visible, and photoluminescence analysis. The result showed that the as-obtained products with the mix of lemon juice (30 ml) and sucrose had a spherical morphology with the mean particle size of about 21.5 nm. The photocatalytic activity of this sample was tested for the degradation of methyl orange, methyl red and methylene blue solutions. The results also revealed the good photocatalytic activity for the degradation of these three organic dyes. Furthermore, as synthesized samples were used in decolourization processes and the treatment of textile dyes.
2. **Umaralikhan *et.al.*, (2016)** investigated that the Zinc oxide nanoparticles (ZnO NPs) and Magnesium doped ZnO nanoparticles (Mg doped ZnO NPs) were synthesized by *Psidium guajava* leaf extract. X-ray diffraction studies confirmed that synthesized nanoparticles retained the hexagonal structure. In FESEM and HRTEM image analysis, ZnO and Mg doped ZnO NPs morphology were of trigonal and spherical shape. Elemental compositions were identified by EDAX analysis. From the FTIR result, the Zn–O stretching was observed at 453 and 448 cm^{-1} for both ZnO samples. In Raman spectra, the high intensive E2 high mode is observed for 438 cm^{-1} for ZnO NPs. But Mg doped ZnO NPs intensity of E2 high mode decreased as compared to the pure ZnO NPs, it is due to the Mg^{2+} ion into ZnO lattice site. The photoluminescence measurements revealed that the broad emission was composed of seven different bands due to zinc vacancies, oxygen vacancies and surface defects.
3. **Mansoore Hosseini Koupaei *et.al.* ,(2016)** reported on the use of coffee powder extract in the biosynthesis of ZnO nanoparticles. Furthermore, the effect of

calcination time (in 600°C) on the size of ZnO nanoparticles was investigated. The samples were characterized using TEM, SEM, EDAX, XRD, and FT-IR. Then, the influence of green synthesized ZnO nanoparticles calcined at 600°C for 2h on proteinase K was investigated. The enzyme activity of Proteinase K showed that ZnO nanoparticles inhibited the activity of the enzyme and its thermal stability was increased by enhancing the concentration of nanoparticles.

4. **Gnanasangeetha. et.al., (2013)** reported the exploit of aqueous leaf extract of *Coriandrum sativum* as an eco-friendly agent for the preparation of Zinc Oxide nanoparticle using zinc acetate and sodium hydroxide as a surrogate for Chemical method. The characterization of ZnO nanoparticles prepared by green and chemical techniques (XRD, SEM, FTIR and EDAX). ZnO nanoparticles have found fabulous application in biomolecular detection, diagnostics, microelectronics and water remediation.
5. **Yuvakkumar et.al., (2014)** prepared zinc oxide nanoparticles effectively from *Nephelium lappaceum L.* peels. The role of extract on the formation of zinc oxide nanoparticles was confirmed by employing HPLC and GC-MS studies. The XRD and TEM revealed the crystallinity and spherical morphology of the biosynthesized nanoparticles. The size of the particles was found to be 20 nm as deduced from XRD and TEM analysis.
6. **Gunabalan Madhumitha et.al., (2015)** have elaborated on various natural source-mediated Synthesis of ZnO NPs and their role in various biological activities like antimicrobial, cytotoxic, and photocatalytic activities. Apart from these applications, ZnO NPs were also reported to help to prevent dust formation, for several years, on oil paintings.
7. **Sundrarajan et.al., (2015)** synthesized ZnO nanoparticles using *Pongamia pinnata* leaves extract and were characterized by XRD, UV-vis, DLS, SEM, TEM and FT-

IR spectroscopy. The synthesized ZnO nanoparticles were confirmed by XRD and FTIR spectra. Morphology studies indicate the spherical nature of the ZnO NPs and EDX shows the highly pure ZnO nanoparticles. The antibacterial activity of ZnO nanoparticles and ZnO nanoparticles coated cotton fabric were tested against *Staphylococcus aureus* (gram positive) and *Escherichia coli* (gram negative) organisms by agar diffusion method. Finally, the current study has clearly demonstrated that the ZnO NPs are responsible for significant higher antibacterial activities. Therefore, the study reveals an efficient, eco-friendly and simple method for the green synthesis of multifunctional ZnO NPs using a green synthetic approach.

8. **Thema *et.al.*, (2015)** synthesized ZnO nanoparticles by using *Agathosma betulina* plant extract as an effective chelating agent. The surface/interface and volume room temperature properties of these quasi- spherical 15.8 nm in size ZnO nanoparticle by transmission electron microscopy, energy dispersive X-Ray Spectroscopy, X-rays diffraction, attenuated total reflection IR and Raman spectroscopy are reported.
9. **Suresh *et.al.*, (2015)** synthesized ZnO nanoparticles by using aqueous *Cassia fistula* plant extract as fuel by solution combustion synthesis. The ZnO Nps were characterized by Powder X- ray diffraction (PXRD), UV–visible studies and Transmission electron microscopy (TEM). The Nps were evaluated for photodegradation, antimicrobial and antioxidant activities.
10. **Fatimah *et.al.*, (2016)** investigated for obtaining ZnO nanoparticles via complex formation with plant extracts. *Mimosa pudica* leaves and coffee powder were utilized as template for synthesis of ZnO nanoparticles. After the complex formation, calcination of the complexes at the temperature related to thermal transformation was conducted. DTA-TGA, XRD and DRUV-Vis spectrophotometric analysis were utilized to study the effect of synthesis route to the physicochemical character and methylene blue photooxidation was chosen as a reaction model to evaluate the photoactivity. The results show that the materials

have crystallite size of around 27.14 Å and 46.94 Å from the utilization of *Mimosa pudica* and coffee powder extracts respectively.

11. **Vidya et.al., (2013)** synthesized ZnO nanoparticles by zinc nitrate and utilizing the bio components of leaves extract of *Calotropis Gigantea*. The ZnO nano crystallites have an average size range of 30-35 nm. Zinc nanoparticles were characterized using SEM and XRD. The particles obtained are spherical in nature. The X ray patterns show hexagonal crystal type for ZnO. The results coincide with the literature XRD pattern for hexagonal wurtzite ZnO. The size of nano crystallites is calculated by considering XRD data by Debye-Scherrer's Formula.
12. **Ambika et.al., (2015)** synthesized ZnO nanoparticles using *Vitex negundo* plant extract with zinc nitrate hexahydrate as precursor. Presence of isoorientin (flavone) in *Vitex negundo* plant extract is mainly responsible for the formation of ZnO NPs. The prepared ZnO NPs were calcinated at 450°C and were confirmed by XRD, FT-IR, UV-visible, SEM with EDX and DLS analysis. The biological application of antibacterial activity was done by gram positive and gramnegative bacteria..
13. **Kavita Vishwakarma et.al., (2013)** synthesized ZnO nanoparticles using the aqueous solution of *Abrus precatorius* seeds extract and zinc acetate. A fixed ratio of plant extract to metal ion was prepared and the color change was observed which proved the formation of nanoparticles. The nanoparticles were characterized by UV-vis Spectrophotometer, FTIR, DLS, Zeta Analysis, XRD, and SEM. The particles synthesized were of the size ranging from 90-500 nm.
14. **Li Fu and Zhuxian Fu et.al., (2015)** reported the synthesis of ZnO nanoparticles (NPs) using leaf extract of *Plectranthus amboinicus*. The synthesized ZnO NPs were characterized by UV-vis spectroscopy, SEM, EDX, XRD, FTIR and photoluminescence spectroscopy. SEM study reveals that the biosynthesized ZnO NPs exhibit a rod shape structure with an average size of 88 nm. The UV-vis diffuse reflectance spectrum study indicates the band gap of biosynthesized ZnO NPs is 3.07 eV. Photocatalytic property of the ZnO NPs was investigated by

photodegradation of methyl red (MR) under UV illumination. The photocatalytic performance of biosynthesized ZnO NPs was compared with hydrothermal synthesized ZnO NPs and P25. Results show that the biosynthesized ZnO NPs owing a superior photocatalytic activity towards degradation of MR.

15. **Majid Darroud *et.al.*, (2013)** reported the “green”and biosynthesis of zinc oxide nanoparticles (ZnO-NPs) using gum tragacanth. Spherical ZnO-NPs were synthesized at different calcination temperatures. TEM imaging showed the formation of most nanoparticles in the size range of below 50 nm.The powder X-ray diffraction (PXRD) analysis revealed wurtzite hexagonal ZnO with preferential orientation in (101) reflection plane. In vitro cytotoxicity studies on neuro2A cells showed a dose dependent toxicity with non-toxic effect of concentration below 2 mg/mL.

16. **Manuela Stan *et.al.*, (2015)** prepared the ZnO nanoparticles using aqueous extracts of *Allium sativum* (garlic), *Allium cepa* (onion) and *Petroselinum crispum* (parsley)For all ZnO samples, the XRD studies reveal a hexagonal wurtzite structure, without supplementary diffraction lines. The particle size is influenced by the type of plant extract used and varies between 14 and 70 nm. The biomolecules involved in the biosynthetic procedure was evidenced by FTIR spectroscopy. Also, Zn vacancy complexes and oxygen vacancies are present in all analyzed samples. A narrowing of the band gap for the ZnO prepared with plant extracts was observed as compared to that of the ZnO, prepared using solely ultrapure water. The photodegradation studies conducted in the presence of UV light irradiation indicated that ZnO nanoparticles prepared using garlic extract exhibit the highest efficiency in the photodegradation of methylene blue dye.

17. **Ochieng *et.al.*, (2015)** reported that the zinc oxide nanoparticles (ZnO NPs) were successfully synthesized using zinc nitrate and aqueous leaf extract of *Spathodea campanulata* as the reducing as well as stabilizing agent. Formation of nanoparticles was monitored using UV-Visible spectroscopy and a characteristic

absorption peak at 328nm was observed. From the TEM images, the synthesized ZnO nano-crystallites were of uniform morphology and size range of 20-50 nm. XRD characterization revealed the face-centered cubic of highly crystalline nanoparticles. SEM images revealed spherically shaped and smooth surfaced nanoparticles arranged on top of one another. The EDX gave strong signals for zinc and oxygen at energies 137.6888 units and 118.0190 units, respectively, indicating the occurrence of the nanoparticles in their oxide form rather than the pure zinc form. From the FTIR spectra of the zinc oxide nanoparticles, the characteristic absorption peak of the Zn-O bond was observed at 848cm^{-1} . The spectra of the *Spathodea campanulata* extract gave an O-H stretch of polyphenols at 3222cm^{-1} , nitrile group from proteins at 2339cm^{-1} and double substituted aromatic bending at 682cm^{-1} .

18. **Saranya *et.al.*, (2017)** synthesized ZnO NPs using the extract of *Zea mays* and zinc sulfate solution respectively. The synthesized nanoparticles were characterized by UV-visible spectrophotometer, XRD, FTIR, SEM, TEM, AFM and Zeta potential particle size analyzer. Optimum parameters such as precursor salt solution concentration, pH, ratio between reducing agent and precursor salt solution and reaction time, the formation and stability of the reduced metal nanoparticles in the colloidal solution were monitored by UV-visible spectrophotometer analysis. The mean particle diameter of nanoparticles were calculated from the XRD pattern according to the line width of the plane, reflection peak using the Scherrer's equation. FTIR results suggested that possible biomolecules for the reduction of metallic nanoparticles. SEM and TEM analysis showed the formation of well dispersed metallic nanoparticles and the synthesized metallic nanoparticles were in nano scale range. Antimicrobial activities of the metallic nanoparticles were performed by a well diffusion method against *Escherichia coli*, *Staphylococcus aureus*, *Streptococcus agalactiae* and *Salmonella enterica*.

19. **Karnan *et.al.*, (2016)** synthesized the ZnO nanoparticles from rambutan (*Nephelium lappaceum*L.) peel extract via bio synthesis method. During the

synthesis, fruit peel extract acts as a natural ligation agent. The successfully prepared product was analyzed with some standard characterization studies like XRD, UV-Vis DRS, FESEM, HR-TEM, N₂ adsorption-desorption isotherm and UV-Visible absorption Spectroscopy. The photocatalytic activity of ZnO nanoparticles was evaluated by photodegradation of methyl orange (MO) dye under UV light and the result depicts around 83.99% decolorization efficiency at 120 minutes of illumination. In addition with photo decolorization, mineralization was also achieved. The mineralization has been confirmed by 33 measuring Chemical Oxygen Demand (COD) values.

20. **Diallo *et.al.*, (2015)** reported for the 1st time on the synthesis and the main physical properties of ZnO nanoparticles synthesized by an entirely green physical-chemistry process using *Aspalathus linearis*'s natural extract as an efficient reduction/oxidizing agent. Their structural and optical properties by electron microscopy, X-rays diffraction, Raman and X-rays photoemission spectroscopies as well as room temperature photoluminescence are reported.
21. **Gawade *et.al.*, (2017)** demonstrated a facile, innovative and inexpensive green route for the formation of ZnO nanoparticles by biogenic method using aqueous leaf extract of *Calotropis procera* which acts as a reducing and stabilizing agent. The prepared ZnO nanoparticles were characterized by a host of different techniques such as XRD, DRS, TEM and FT-IR. The XRD pattern confesses that ZnO nanoparticles are associated with hexagonal wurtzite structure. The DRS absorption spectrum shows an absorption edge at 397 nm corresponds to the ground excitonic peak of ZnO nanoparticles and the band gap is found to be 3.1 eV. The FT-IR spectra indicate the presence of various compounds which are responsible for biochemical reaction. TEM images show that the particles of ZnO have spherical shape with size ranging from 15 to 25 nm.
22. **Vijayakumar *et.al.*, (2016)** reported the green synthesis of zinc oxide nanoparticles using the aqueous leaf extract of *Laurus nobilis* by co-precipitation

method. The synthesized ZnO NPs were characterized by UV–Vis spectroscopy, FTIR, XRD, TEM, SEM and EDX. *Ln-ZnO* NPs were crystalline in nature, flower-like and have hexagonal wurtzite structure with a mean particle size of 47.27 nm. The antibacterial activity of *Ln-ZnO* NPs was greater against Gram positive (*Staphylococcus aureus*) bacteria than Gram negative (*Pseudomonas aeruginosa*) bacteria.

23. **Rajeswari Rathnasamy et.al.,(2017)** prepared the wurtzite ZnO nanoparticles through green synthesis method using *Carica papaya* leaf extract. To understand the structural phase purity, morphology and size, the sample was characterized through various analytical techniques. The obtained results reveal that the synthesized ZnO nanoparticle is a phase pure hexagonal wurtzite structure in spherical shape with particle size of ~50 nm. Furthermore, the synthesized ZnO nanoparticles were used as photocatalyst as well as photo anode for methylene blue dye degradation and dye sensitized solar cells, respectively. It was found that the synthesized ZnO nanoparticles completely degrade the methylene blue dye within 180 min under UV light irradiation. In addition, it shows an energy conversion efficiency of 1.6% with a current density of 8.1 mA cm⁻² in dye sensitized solar cells.
24. **Sagar Raut et.al., (2015)** discussed the synthesis and characterization of ZnO nanoparticles by green synthesis method. There they utilized the leaves of *Ocimum Tenuiflorum* plant as a reducing agent in the synthesis of ZnO nanoparticles. Green synthesis method avoids inert gases, high pressure, laser radiation, high temperature, toxic chemicals etc. as compared to conventional methods like sol-gel technique method, laser ablation method, solvothermal method, inert gas condensation method, chemical reduction method etc. Prepared ZnO nanoparticles were characterized by XRD, SEM and FTIR. The average particle are calculated as 13.86 nm by using Scherrer's formula.

25. **Pavan Kumar et.al., (2015)** reported the multifunctional zinc oxide nanoparticles (ZnO Nps) were synthesized by solution combustion synthesis using beetroots (*Beta vulgaris*). The structure and morphology of the product were studied by powder XRD, UV-visible spectroscopy and SEM. XRD studies indicate the formation of Nps with hexagonal wurtzite structure having crystallite sizes in the range of ~ 52–76 nm. The UV-visible spectrum of Nps shows maximum absorption at 373 nm. The SEM analysis indicates the formation of porous, sponge-like agglomerated structures. ZnO Nps effectively degrades malachite green (MG) and methylene blue (MB) dyes in the presence of UV light. Nps show good antioxidant activity by scavenging 1,1-Diphenyl-2-picrylhydrazyl (DPPH) radicals. The study successfully demonstrates simple, economical and ecofriendly methods of synthesis of multifunctional ZnO Nps. Nps may be used as good color tunable phosphor materials.
26. **Nethravathi et.al., (2015)** prepared the multifunctional zinc oxide nanoparticles (ZnO Nps) by using the water extract of *Garcinia xanthochymus* by solution combustion synthesis. The structure and morphology were determined by XRD, UV-visible and SEM studies. The ZnO Nps were evaluated for photoluminescence (PL), photocatalytic and antioxidant properties. Powder XRD studies indicate the formation of pure wurtzite structure with absorption maximum of 370 nm corresponding to band gap energy of 3.33 eV. SEM studies reveal the formation of spongy cave like structures. The PL spectra exhibited 4 emission edges at 397, 436, 556 and 651 nm upon excitation at 325 nm because of oxygen deficiencies and zinc interstitials.
27. **Matias et.al., (2017)** synthesized Zinc oxide nanoparticles through green method using *Moringa Oleifera* extract as an effective chelating agent. The electrochemical activity, crystalline structure, morphology, isothermal behavior, chemical composition and optical properties of ZnO nanoparticles were studied using various characterization techniques i.e CV, XRD, HRTEM, SEAD, DSC/TGA, FTIR and (UV-vis). The electrochemical analysis proved that the ZnO

nano has high electrochemical activity without any modifications and therefore are considered as a potential candidate in electrochemical applications. The XRD pattern confirmed the crystallinity and pure phase of the sample. DSC/TGA analysis of the ZnO sample revealed three endothermic peaks around 140.8 °C, 223.7 °C and 389.5 °C.

28. **Nagaraju *et.al.*, (2017)** reported the formation of unique morphologies of zinc oxide (ZnO) super structured frameworks via a simple and eco-friendly route employing PL, SEM and TEM studies are performed to analyze the formation and characterization of ZnO. XRD confirmed the crystalline nature of the material with hexagonal Wurtzite structure having average crystallite size of ~50 nm. FTIR spectrum shows a band at 532 cm⁻¹ due to the vibrational mode of Zn-O bending. TEM images clearly show lattice spacing of 0.29 nm corresponding to the (002) plane of ZnO. Photoluminescence (PL) spectrum shows strong yellow light emission upon excitation at 320 nm due to the Zn-O defects. Synthesized ZnO nanoparticles (Nps) exhibited good photocatalytic activity for the degradation of Methylene blue (MB) dye. ZnO Nps also exhibited superior antibacterial activity against *Staphylococcus aureus* and *Escherichia coli* bacteria.

29. **Subramani Karthik *et.al.*, (2017)** synthesized the ZnO nanoparticles from *Acalypha indica* leaf extract using zinc acetate as a precursor. The prepared ZnO nanoparticles were calcined at three different temperatures, namely 100, 300, and 600 °C. The structure/morphology of the green-synthesized ZnO nanoparticles was ascertained through XRD, particle size analysis, SEM, TEM and surface area analysis techniques. It was observed from the physico-chemical and biological characterization studies that ZnO nanoparticles calcined at high temperature (600 °C) exhibit high surface area (230 m² g⁻¹) and small particle size (20 nm) with good antibacterial activity against *Escherichia coli* (22.89 ± 0.06 mm) and *Staphylococcus aureus* (24.62 ± 0.08 mm).

30. **Saad S M Hassan *et.al.*, (2015)** prepared the Zinc oxide nanoparticles using *Coriandrum sativum* leaf extract and zinc acetate dihydrate. It was utilized as a photocatalyst for the degradation of anthracene. The catalyst was characterized by XRD, SEM, TEM, Raman spectroscopy and UV–vis spectrophotometry.
31. **Chinnammal Janaki *et.al.*, (2015)** reported the green synthesis of ZnO nanoparticles by Zinc Carbonate and utilizing the bio-components of powder extract of dry ginger rhizome (*Zingiber officinale*). The ZnO nano crystallites have an average size range of 23–26 nm. Zinc oxide nanoparticles were characterized by using XRD, SEM, EDX. FTIR spectra confirmed the adsorption of surfactant molecules at the surface of ZnO nanoparticles and the presence of ZnO bonding. Antimicrobial activity of ZnO nanoparticles was done by a well diffusion method against pathogenic organisms like *Klebsiella pneumonia*, *Staphylococcus aureus* and *Candida albicans* and *Penicillium notatum*. It is observed that the ZnO synthesized in the process has efficient antimicrobial activity.
32. **Momeni *et.al.*, (2016)** prepared the ZnO nanoparticles (NPs) using *Euphorbia prolifera* leaf extract as a non-toxic reducing agent and efficient stabilizer without using dangerous, hazardous and toxic materials. The approach of biosynthesis appears to be a cost efficient, eco-friendly and easy alternative to conventional methods of the ZnO NPs synthesis. The ZnO NPs were characterized by FESEM, EDS, elemental mapping, TEM and XRD. TEM micrograph has shown the formation of Cu NPs with the size in the range of 5–17 nm. In addition, the synthesized ZnO NPs presented excellent catalytic activity for the degradation of Methylene blue (MB) and Congo red (CR) in the presence of NaBH₄ in water at room temperature.
33. **Senthilkumar *et.al.*, (2014)** synthesized the Zinc oxide nanoparticles (ZnO Nps) using the aqueous extract of green tea (*Camellia sinensis*) leaves. The UV-Vis spectrum was recorded to monitor the formation of the nanoparticles, which exhibited a blue shifted absorption peak at 325 nm. The XRD pattern revealed the

hexagonal wurtzite structure of ZnO nanoparticles. FT-IR spectra were recorded for the green tea extract and for the ZnO nanoparticles to identify the biomolecules involved in the synthesis process.

34. **Vidya et.al., (2017)** used the *Artocarpus Heterophyllus* leaves extract for the synthesis of Zinc oxide nanoparticles (ZnO NPs). The particles were calcined at 400, 600 and 800 °C for 1 h. Powder X-Ray Diffraction (PXRD) results showed the ZnO NPs calcined at different temperatures to be crystalline with hexagonal wurtzite phase. The morphology was studied using SEM and elemental composition investigated using EDS showed peaks for Zn and O only. The exact size of ZnO particles and its crystalline nature were investigated from TEM, High resolution transmission electron microscopy (HRTEM) and selected area electron diffraction (SAED).
35. **Archana et.al., (2017)** prepared the ZnO nanoparticles using *Moringa Oleifera* natural extract. XRD and Raman analysis show crystalline ZnO with wurtzite structure. SEM and TEM images show the average size of the nanoparticles to be 100–200 nm. Photocatalytic generation of hydrogen by these nanoparticles has been investigated under UV–Visible light irradiation.
36. **Taghavi Fardood et.al., (2017)** synthesized the , zinc oxide (ZnO) nanoparticles using arabic gum as a biotemplate source by the sol–gel method and its photocatalytic dye degradation ability from aqueous solution was studied. This method has many advantages such as nontoxic, economic viability, ease to scale up, less time consuming and environmentally friendly approach for the synthesis of ZnO nanoparticles without using any organic chemicals. Direct blue 129 (DB129) was used as model dye. The synthesized ZnO nanoparticles were characterized by powder XRD, FTIR, SEM and UV–Visible spectroscopy. The X-ray powder diffraction (XRD) analysis revealed the formation of wurtzite hexagonal phase ZnO with average crystallite size of 10 nm. Photocatalytic dye degradation by ZnO nanoparticles was studied using UVVis spectrophotometer.

37. **Siripireddy Balaji and Mandal Badal Kumar *et.al.*, (2017)** used the *Eucalyptus globulus* leaf extract mediated synthesis of spherical zinc oxide nanoparticles (ZnO NPs). UV–Visible studies of the synthesized nanoparticles revealed the characteristic peak at 361 nm indicating the formation of ZnO nanoparticles. Powder XRD study showed the strong, intense and narrow-width diffraction peaks indicating the formation of crystalline nanoparticles with the most stable hexagonal phase. FE-SEM and HR-TEM results confirmed the formation of spherical ZnO NPs with mean particle size of 11.6 nm which is in close agreement with the XRD pattern. Further, EDAX revealed the formation of highly pure ZnO NPs with the peaks of Zn and O atoms. ZnO NPs exhibited effective photocatalytic activity in degrading Methylene blue and Methyl orange with maximum degradation efficiency up to 98.3% at 30 mg of catalyst doses. In addition, ZnO NPs exhibited high antioxidant activity against DPPH free radical scavengers.
38. **Xueshan Li *et.al.*, (2013)** The zinc oxide (ZnO)-reduced graphene oxide (RGO) nanocomposites were greenly synthesized by one-step hydrothermal reaction with ZnCl₂ and graphite oxide (GO) as precursors without extra reductant. It was validated that the ZnO spherical particles assembled by ZnO nanorods with an average diameter of 150 nm are uniformly deposited on the RGO sheets. Meanwhile, due to the introduction of RGO, the light adsorption scope of ZnO is enlarged, the size of ZnO is decreased, the degree of crystallinity is improved and the self-aggregation of the ZnO particles is effectively prevented. Compared with the pure ZnO particles, the efficiency of the nanocomposites for the photo-degradation of RhB is increased by 39% .
39. **Salam *et.al.*, (2014)** reported the synthesis of zinc oxide nanoparticles (ZnO-NPs) using *Ocimum basilicum* L. var. *purpurascens* Benth.-Lamiaceae leaf extract and zinc nitrate. Hexagonal (wurtzite) shaped ZnO-NPs with size about 50 nm were synthesized and characterized using XRD, TEM and EDX analysis.

40. **Nava et.al., (2017)** synthesized the Zinc Oxide nanoparticles using different amounts of *Camellia sinensis* extract. The Synthesized material was studied and characterized through FTIR, XRD, TEM. The Zinc Oxide nanoparticles presented the desired ZnO bond at 618 cm^{-1} , demonstrated growth in a purely hexagonal Wurtzite crystal structure, and, depending on the amount of extract used, they presented different size and shape homogeneity. The photocatalytic activity of the obtained Zinc Oxide nanoparticles was studied. The photocatalytic degradation studies were done at a 1:1 M ratio of methylene blue to Zinc Oxide nanoparticles under UV light.
41. **Nava et.al., (2017)** presented a study of the effects on the photocatalytic capabilities of zinc oxide nanoparticles when prepared via green synthesis using different fruit peel extracts as reducing agents. Zinc nitrate was used as a source of the zinc ions, while *Lycopersicon esculentum* (tomato), *Citrus sinensis* (orange), *Citrus paradisi* (grapefruit) and *Citrus aurantifolia* (lemon) contributed their peels for extracts. The Synthesized Samples were studied and characterized through FTIR, XRD, and HRTEM. All samples presented a band at 618 cm^{-1} , indicating the presence of the ZnO bond. The different samples all presented the same hexagonal crystal growth in their structure, the Wurtzite phase. The surface morphology of the nanoparticles showed that, depending on the extract used, the samples vary in size and shape distribution due to the chemical composition of the extracts. The photocatalytic properties of the zinc oxide samples were tested through UV light aided degradation of methylene blue.
42. **R.Sharmila Devi and R. Gayathri et.al., (2014)** synthesized the Zinc Oxide nanoparticles by Zinc nitrate and utilizing the bio components of leaves extract of *Hibiscus rosa-sinensis*. The particle size and morphology of the synthesized

nanoparticles is characterized by using Scanning Electron Microscope (SEM), and X-ray Diffraction (XRD).

43. **A Singh, et al *et.al.*, (2016)** synthesized the zinc oxide nanoparticles (ZnO NPs) by treating zinc acetate dihydrate with the flower extract of *Elaeagnus angustifolia* (Russian olive). The formation of ZnO NPs was primarily confirmed by UV–visible absorption spectrum in the range of 250–700 nm. XRD analysis and DLS particle size analyzer revealed the size of ZnO NPs. The FTIR spectrum revealed the presence of phytochemicals in the flower extract mediated ZnO NPs. Moreover, the morphology of the ZnO NPs was determined using SEM. Seeds of *Solanum lycopersicum* (tomato) were separately treated with different concentrations of synthesized ZnO NPs and zinc sulfate (ZnSO₄) salt suspensions (common zinc supplement). The effect of these treatments on seed germination, seedling vigor, chlorophyll, protein and sugar contents as well as on the activities of lipid peroxidation and antioxidant enzymes were studied. The effect of synthesized ZnO NPs on seedling vigor, pigment, protein and sugar content was found affirmative at lower concentrations contrary to control and ZnSO₄ salt. To the best of our knowledge this is the first report on *Elaeagnus angustifolia* mediated synthesis of ZnO NPs and their effects on germination and physiological activity of tomato.

44. **Rajaboopathy and S. Thambidurai *et.al.*, (2017)** reported the Green synthesis of seaweed-macro algae based cadmium oxide-zinc oxide (SCZ) nanoparticles was prepared by the simple chemical precipitation method. The functional group characteristics and crystalline properties of the nanoparticles were analyzed by FTIR and XRD analysis. The optical band gap energy of SCZ nanoparticles showed a lower value (3.11 eV), these can be due to the incorporation of seaweed (SW) and cadmium oxide (CdO). Small fiber like seaweed constituent was entangled over the CdO-ZnO nanoparticles, these were confirmed with High resolution scanning electron microscope and Field emission gun-transmission electron microscope analysis. The particle size of SCZ nanoparticles was obtained in the range of 20–50 nm.

45. **Thenmozhi, et.al., (2017)** synthesized the ZnO nanoparticles from green tea leaves (*Camellia sinensis*). The formation of nanoparticles was observed by visualizing color changes and it was confirmed by SEM, UV-Vis spectrophotometer and FT-IR spectrophotometer. The results of various techniques confirmed the presence of Zinc oxide nanoparticles. The UV-Vis spectrum was recorded to observe the absorption spectra, which exhibited a blue shift absorption peak at 338 nm. The XRD pattern revealed well-defined peaks appearing at 2θ positions corresponding to the hexagonal wurtzite structure of ZnO nanoparticles. The average size of the nanoparticles calculated using XRD data was 54.84 nm. FT-IR spectra were recorded for the as-prepared nanoparticle to identify the biomolecules involved in the synthesis process. CV study shows an excellent capacitance behavior, low equivalent series resistance (ESR) and fast diffusion of electrolyte ions into the composite. This confirms that the as-prepared ZnO material is the best suitable material for supercapacitor applications.
46. **Elumalai et.al., (2015)** reported a simple and eco-friendly method for the synthesis of zinc oxide nanoparticles (ZnO NPs) using leaf extract of *Moringa oleifera*. The prepared ZnO NPs were characterized various techniques such as UV-Vis absorption spectroscopy, XRD, FE-SEM, EDX, FT-IR and PL. XRD analysis revealed the wurtzite hexagonal structure of ZnO NPs. FT-IR confirmed the presence of Functional groups of both leaf extract and ZnO NPs. The particles size, morphology and topography determined from FE-SEM. The intense and narrow width of zinc and oxygen have high purity and crystalline were identified using EDX. UV-Visible absorption showed the characteristic absorption peak of ZnO NPs. The results of antimicrobial activities revealed that the maximum zone of inhibition was observed against gram (+ve) positive bacteria and followed by the gram (-ve) negative bacteria at concentration of 200 $\mu\text{g/mL}$ of ZnO NPs.
47. **Prasanta sutradhar and mitali saha et.al., (2015)** reported the green synthesis of zinc oxide nanoparticles (ZnONPs) by thermal method and under

microwave irradiation using the aqueous extract of tomatoes as non-toxic and reducing material. The synthesised ZnONPs were characterized by UV–vis, FTIR, particle size analyser, SEM, atomic force microscopy (AFM) and XRD. A series of ZnO nanocomposites with titanium dioxide nanoparticles Structural and morphological studies of these nanocomposites were carried out using UV–vis, SEM, XRD and AFM.

48. **Elumalai et.al., (2015)** synthesized zinc oxide nanoparticles (ZnO NPs) from the leaf extract of *Vitex trifolia* L. GC and GC–MS analyses revealed that the *V. trifolia* contained 17 compounds. The synthesized ZnO NPs was characterized by UV–Vis, PL, XRD, FT-IR, SEM, FE-SEM, EDX and TEM techniques. In addition, the antimicrobial activity was evaluated by disc diffusion, MIC, MBC and MFC procedure. The results depicted that the inhibition zone is dependent on the ZnO NPs concentration and green synthesized ZnO NPs had outstanding antimicrobial activity than others (bare ZnO, leaf of *V. trifolia*). The possible reason may due to the Vitrifolin A (major compound of leaf extract) which binds the surface of the nanoparticles increased the antimicrobial activities.
49. **Noorjahan et.al., (2015)** synthesized Zinc oxide nanoparticle using aqueous neem (*Azadirachta indica*) leaf extract. The aqueous leaf extract acts as a solvent with manifold roles as promoter, stabilizer and template for the synthesis of nanoparticles. The synthesized ZnO nanoparticle was characterized using FTIR spectroscopy and SEM analysis. The results of FTIR analysis of green synthesized nanoparticle revealed the presence of biomolecules such as Polyphenols, Carboxylic acid, polysaccharide, amino acids and proteins. The results of the SEM studies of green synthesized ZnO nanoparticle showed the formation of spindle shaped nanoparticles and Zinc oxide nanoflakes.
50. **Niranjan Bala et.al., (2014)** synthesized Zinc oxide (ZnO) nanoparticles (NPs) using *Hibiscus sabdariffa* leaf extract. Temperature dependent synthesis and particle growth have been studied. Formation of NPs was confirmed by UV-VIS,

FTIR and XRD. Electron microscopy has been used to study the morphology and size distribution of the synthesized particles. The synthesized ZnO nanoparticles as potential anti-bacterial agents have been studied on *Escherichia coli* and *Staphylococcus aureus*. Another study has indicated that small sized ZnO NPs, stabilized by plant metabolites, had better anti-diabetic effect on streptozotocin (STZ) induced diabetic mice than that of large sized ZnO particles. It has also been observed by enzyme linked immunosorbent assay (ELISA) and real time polymerase chain reaction (RT-PCR) that ZnO can induce the function of Th1, Th2 cells and expressions of insulin receptors and other genes of the pancreas associated with diabetes.

51. **Bhuvaneswari et.al., (2017)** prepared the zinc oxide nanoparticles (ZnONps) using domestic waste-starch rich potato peel and zinc oxide powders. The particle size and morphology of the synthesized nanoparticles is characterized by using UV VIS spectrophotometer, FTIR and SEM analysis. The effluents were treated with ZnONps and the photocatalytic degradation capability of the dyes significantly enhanced the great potential for wastewater treatment system.

52. **Sadhan Kumar Chaudhuri & Lalit Malodia et.al., (2017)** reported the Green synthesis of zinc oxide nanoparticles using *Calotropis* leaf extract with zinc acetate salt in the presence of 2 M NaOH. The combination of 200 mM zinc acetate salt and 15 ml of leaf extract was ideal for the synthesis of less than 20 nm size of highly monodisperse crystalline nanoparticles. Synthesized nanoparticles were characterized through UV–Visible spectroscopy, DLS, XRD, SEM, EDX, and AFM. Effects of biogenic zinc oxide (ZnO) nanoparticles on growth and development of tree seedlings in the nursery stage were studied in open-air trenches. The UV– Visible absorption maxima showed a peak near 350 nm, which is characteristic of ZnO nanoparticles. DLS data showed that single peak is at 11 nm (100%) and the Polydispersity Index is 0.245. XRD analysis showed that these are highly crystalline ZnO nanoparticles having an average size of 10 nm. FTIR spectra

were recorded to identify the biomolecules involved in the synthesis process, which showed absorption bands at 4307, 3390, 2825, 871, 439, and 420 cm^{-1} . SEM images showed that the particles were spherical in nature. The presence of zinc and oxygen was confirmed by EDX and the atomic % of zinc and oxygen were 33.31 and 68.69, respectively. 2D and 3D images of ZnO nanoparticles were obtained by AFM studies, which indicated that these are monodisperse having size ranges between 1.5 and 8.5 nm. Significant enhancement of growth was observed in Neem (*Azadirachta indica*), Karanj (*Pongamia pinnata*), and Milkwood-pine (*Alstonia scholaris*) seedlings in foliar spraying ZnO nanoparticles to nursery stage of tree seedlings. Out of the three treated saplings, *Alstonia scholaris* showed maximum height development.

53. **Paul et.al., (2017)** reported a novel and green approach for one-pot biosynthesis of zinc oxide (ZnO) nanoparticles (NPs). Highly stable and hexagonal phase ZnO nanoparticles were synthesized using seeds extract from the tender pods of *Parkia roxburghii* and characterized by XRD, FT-IR, EDX, TEM, and N₂ adsorption-desorption (BET) studies. The powder XRD pattern furnished evidence for the formation of hexagonal close packing structures of ZnO NPs having average crystallite size 25.6 nm. The TEM image reveals rice shapes ZnO NPs are with an average diameter of 40–60 nm. The as-synthesized ZnO NPs has proved to be an excellent sono catalysts for degradation of organic dye and synthesis of 2-benzimidazole derivatives.

54. **Nagajyothi et.al., (2017)** synthesized the zinc oxide nanoparticles (ZnO NPs) using the root extract of *Polygala tenuifolia*. Synthesized ZnO NPs were characterized by UV– Visible spectroscopy, FTIR, TGA, TEM, SEM and EDX. Anti-inflammatory activity was investigated in LPS-stimulated RAW 264.7 macrophages, whereas antioxidant activity was examined using a DPPH free radical assay. ZnO NPs demonstrated moderate antioxidant activity by scavenging 45.47% DPPH at 1 mg/mL and revealed excellent anti-inflammatory activity by dose-

dependently suppressing both mRNA and protein expressions of iNOS, COX-2, IL-1 β , IL-6 and TNF- α .

55. **Khalil *et.al.*, (2017)** synthesized the zinc oxide (ZnO) nanoparticles via aqueous leaf extracts of *Sageretia thea*. Nanoparticles of size approximately 12.4 nm were extensively characterized. In vitro antimicrobial, cytotoxic, biocompatible and enzyme inhibition assays were performed. Significant antimicrobial activities with and without UV illumination are reported. Bioinspired ZnO nanoparticles were found effective against fungal strains. MTT assay was performed to check the leishmanicidal activity against promastigotes (IC₅₀: 6.2 μ g/ml) and amastigotes (IC₅₀: 10.87 μ g/ml) of *Leishmania tropica*. Brine shrimp lethality was also indicated by bioinspired ZnO nanoparticles (IC₅₀: 21.29 μ g/ml). Hemocompatible nature of bioinspired nanoparticles was revealed. Furthermore, the antioxidant activities were performed. In addition, significant protein kinase while insignificant alpha amylase inhibition were recorded.
56. **Rana *et.al.*, (2016)** reported the green synthesis of ZnO nano-sized spherical particles (ZnO-NPs) using aqueous fruits extract of *Terminalia chebula*. The Structural, morphological and optical properties of green-synthesized ZnO-NPs are characterized by XRD, FTIR, FESEM, UV-Vis and PL spectroscopy techniques. The results show that the synthesized nanoparticles have stable hexagonal wurtzite structure, and are roughly spherical in shape. To explore the photocatalytic activity of the ZnO-NPs the photocatalytic degradation of rhodamine B (RhB) dye is investigated. The results reveal that ZnO-NPs prepared through the green synthesis route are found to be efficient in the degradation of RhB dye.
57. **Namvar, *et.al.*, (2016)** synthesized the zinc oxide nanocomposite using the seaweed *Sargassum muticum* water extract and hyaluronan biopolymer. The morphology and optical properties of the hyaluronan/zinc oxide (HA/ZnO)

nanocomposite were determined by FTIR, XRD, FESEM, TEM and ultraviolet–vis analysis. Electron microscopy and XRD analysis showed that the zinc oxide nanoparticles were polydisperse with a mean size of 10.2 ± 1.5 nm. The nanoparticles were mostly hexagonal in crystalline form. The HA/ZnO nanocomposite showed the absorption properties in the ultraviolet zone that is ascribed to the band gap of zinc oxide nanocomposite. Cytotoxicity studies were also employed.

58. **Azizi, et.al., (2017)** synthesized the ZnO-NPs using zinc nitrate and *Citrullus colocynthis* (L.) Schrad (fruit, seed and pulp) extracts as bio-fuels is reported. The structure, optical, and colloidal properties of the synthesized ZnO-NP samples were studied. Results illustrate that the morphology and particle size of the ZnO samples are different and depend on the bio-fuel. The XRD results revealed that hexagonal wurtzite ZnO-NPs with mean particle size of 27–85 nm were produced by different biofuels. The optical band gap was increased from 3.25 to 3.40 eV with the decreasing particle size. FTIR results showed some differences in the surface structures of the as-synthesized ZnO-NP samples. Furthermore, the as-synthesized ZnO-NPs inhibited the growth of medically significant pathogenic gram-positive (*Bacillus subtilis* and Methicillin-resistant *Staphylococcus aureus*) and gram-negative (*Pseudomonas aeruginosa* and *Escherichia coli*) bacteria.
59. **Rajendran, K Sengodan et.al.,(2017)** synthesized the zinc oxide nanoparticles from different concentrations of *Sesbania grandiflora* leaf extract (5–20%) using zinc nitrate and ferrous chloride as precursor materials and synthesized nanoparticles were characterized using UV-visible spectrometer, FTIR, X-ray diffraction, and SEM. The results showed that synthesized zinc oxide and iron oxide nanoparticles exhibited UV-visible absorption peaks at 235 nm and 220 nm,

respectively, which indicated that both nanoparticles were photosensitive and the XRD study confirmed that both nanoparticles were crystalline in nature. In addition, FTIR was also used to analyze the various functional groups present in the synthesized nanoparticles. The SEM results reveal that zinc oxide nanoparticles were spherical in shape.

60. **Kokabi et.al.,(2017)** synthesized zinc oxide nanoparticles using the aqueous extract of the red seaweed *Hypnea musciformis*. The morphology, purity and quality of biosynthesized ZnONPs were highly comparable with its commercial counterpart with less toxicity. The MIC and MBC values were evaluated and the potential ecotoxicity of Hy-ZnO NPs against *Artemia salina* was investigated in various concentrations (0, 1, 5, 10, 15, 25 $\mu\text{g/ml}$) and mortality rate in 24 hours was evaluated.
61. **Rajan et.al.,(2016)** synthesized zinc oxide nanoparticles using fungus *Aspergillus fumigatus* JCF. The production of zinc oxide nanoparticles was confirmed by the formation of white aggregates of zinc oxide nanoparticles. The optical properties of the nanoparticles were analyzed using UV–vis spectroscopy. The characteristic functional groups were analyzed using FTIR. Particle size and morphology were analyzed using SEM. Antimicrobial activity of zinc oxide nanoparticles towards both gramnegative bacteria (*Klebsiella pneumoniae*, *Pseudomonas aeruginosa* and *Escherichia coli*) and grampositive bacteria (*Staphylococcus aureus* and *Bacillus subtilis*) were studied using well diffusion method.
62. **Debasree Kundu et.al.,(2014)** synthesized the zinc oxide (ZnO) nanoparticles (NPs) rapidly from zinc sulfate solution at room temperature using a metabolically versatile actinobacteria *Rhodococcus pyridinivorans* NT2. The morphology, structure and stability of the synthesized ZnO NPs were studied using UV–vis, XRD, FTIR, FESEM, EDS, TEM, Zeta potential, and thermogravimetry. The data indicated that the synthesized nanoparticles were moderately stable,

hexagonal phase, roughly spherical with average particle diameter in the range of 100–120 nm. Results obtained on examination of protein expression revealed that cell enzymes and extracellular protein systems of *Rhodococcus* sp. may take part in the synthesis process. Furthermore, the ZnO NPs were coated onto textile fabrics to enhance UV-blocking, self-cleaning and antibacterial properties. The antibacterial effects of these textiles were evaluated using ISO 20743 standard. In addition, ZnO NPs exhibited a preferential ability to kill HT-29 cancerous cells as compared with normal peripheral blood mononuclear cells (PBMCs).

63. **Kumar, et.al., (2014)** synthesized the ZnO-NPs using grapefruit (*Citrus paradisi*) peel extract with particle size ranging from 12 to 72 nm. Structural, morphological, and optical properties of the synthesized nanoparticles have been characterized by using UV- Visible spectrophotometer, TEM, DLS, and FTIR analysis. From the results obtained it is suggested that green ZnO-NPs could be used effectively in environmental safety applications and also can address future medical concerns.
64. **Malaikozhundan et.al., (2017)** reported on the anticancer activity of *Pongamia pinnata* seed extract-fabricated zinc oxide nanoparticles (Pp-ZnO NPs) on human MCF-7 breast cancer cells, antibiofilm activity against bacteria and fungi was also investigated. Nanoparticles were characterized by UV–Visible spectroscopy, XRD, FTIR, SEM and EDX. Pp-ZnO NPs effectively inhibited the growth of Gram positive *Bacillus licheniformis* (zone of inhibition: 17.3 mm) at 25 $\mu\text{g ml}^{-1}$ followed by Gram negative *Pseudomonas aeruginosa* (14.2 mm) and *Vibrio parahaemolyticus* (12.2 mm). Pp-ZnO NPs also effectively inhibited the biofilm formation of *C. albicans* at 50 $\mu\text{g ml}^{-1}$. Cytotoxicity studies revealed that a single treatment with Pp-ZnO NPs significantly reduced the cell viability of breast cancer MCF-7 cells at doses higher than 50 $\mu\text{g ml}^{-1}$. Morphological changes in the Pp-ZnO NPs treated MCF-7 breast cancer cells were observed using phase contrast microscopy. This study concludes that the green synthesized P-ZnO NPs may be used as effective antimicrobial and antibreast cancer agents.

65. **Jafarirad, et.al., (2016)** synthesized the ZnONPs that were produced using zinc nitrate and flesh extract of *Rosa canina* fruit (rosehip) which was used as a precursor. The flesh extract acts as a reducing and capping agent for generation of ZnONPs. The structural, morphological and colloidal properties of the as-synthesized NPs have been confirmed by XRD, SEM, EDX, FT-IR and DLS. In comparison with the CH method, the MI method has some advantages such as significantly short reaction time (within 8 min) owing to the high heating rate and thus the accelerated reaction rate. Both methods led to the synthesis of nearly identical NPs with respect to shape and size according to the results of DLS, XRD and SEM techniques. The possible mechanism for synthesis pathway has been proposed based on FTIR results, XRD patterns, potentiometric data and antioxidant activity. In addition, the antibacterial activity of as-prepared ZnONPs was investigated against several bacteria such as *Listeria monocytogenes*, *Escherichia coli*, *Salmonella typhimurium*.

66. **Azizi, et.al., (2016)** developed the zinc oxide nanoparticles (ZnO-NPs) by a green method using simple precursor from the solution consisting of zinc acetate and the flower extract of *Anchusa italica* (*A. italica*). The crystalline structure of ZnO-NPs was shown using XRD analysis. TEM results showed that ZnO-NPs are hexagonal in shapes with mean particle size of ~ 8 and ~ 14 nm at 100 °C and 200 °C annealing temperatures respectively. The antimicrobial activity of ZnO-NPs towards Gram positive (*Bacillus megaterium* and *Staphylococcus aureus*) and Gram negative (*Escherichia coli* and *Salmonella typhimurium*) pathogens decreased with the increasing of the heat treating temperature.

67. **Rajiv et.al., (2013)** synthesized the zinc oxide nanoparticles from *Parthenium hysterophorus* L. by inexpensive, eco-friendly and simple methods. Highly stable, spherical and hexagonal zinc oxide nanoparticles were synthesized by using different concentrations of 50% and 25% parthenium leaf extracts. Both

the concentrations of the leaf extract act as reducing and capping agent for conversion of nanoparticles. Formation of zinc oxide nanoparticles have been confirmed by UV–Visible absorption spectroscopy, XRD, FT-IR, SEM and TEM analysis with EDX. SEM, TEM and EDX analysis reveals that spherical and hexagonal zinc oxide nanoparticle sizes were 27 ± 5 nm and 84 ± 2 nm respectively and chemical composition of zinc oxide were present. Highest zone of inhibition was observed in 25 $\mu\text{g/ml}$ of 27 ± 5 nm size zinc oxide nanoparticles against *Aspergillus flavus* and *Aspergillus niger*. *Parthenium* mediated zinc oxide nanoparticles were synthesized and proved to be good antifungal agents and environment friendly.

68. **Fowsiya et.al., (2016)** reported the microwave assisted extraction of *Carissa edulis* (*C. edulis*) at 70 °C and 400 W was used to extract the secondary metabolites. Further, the metabolites were used as capping agent and Zn (NO₃)₂ as the metal precursor to synthesize ZnO nanoparticles (ZnO NPs). UV–Vis spectroscopy, FT-IR, XRD, SEM and HR-TEM were used for the characterization of nanoparticles. The Surface Plasmon Resonance around 358 nm from the UV–Vis spectroscopy result represents the ZnO NPs formation. The FT-IR confirms the presence of functional groups that acts as the capping agent for the synthesis of ZnO NPs. The crystalline structure of nanoparticles is revealed in the XRD result, morphology shown by SEM results and the size of the ZnO NPs were predicted by HR-TEM. They have carried out the photocatalytic degradation of Congo red at 365 nm in a photo reactor using ZnO NPs.

69. **Venkateswara Rao, Y.T. Prabhu et.al., (2015)** reported the beneficial effect of zinc oxide nanoparticles having a diameter of 20 nm on (*Vigna radiata* L.) seeds, which has been characterized by XRD, PSA, FTIR, SEM and TG-DTA. The measurements of germination percentage, biomass, shoot and root growth were noted down using with and without nanoparticles.

70. **Mahendiran, et.al., (2017)** synthesized the zinc oxide (ZnO) nanoparticles successfully by using aqueous extracts of *Aloe vera* gel/leaf and *Hibiscus sabdariffa* leaf, and characterized by FT IR, UV-Vis, XRD, SEM, and EDX techniques. Phytochemical screening of the *A. vera* gel and leaf and *H. sabdariffa* leaf extracts showed the presence of secondary metabolites. FT IR spectra showed the presence of functional groups and protein as the stabilizing agent surrounding the ZnO nanoparticles. UV-Vis spectra of ZnO nanoparticles exhibit the characteristic absorption band in the range of 344–360 nm, which can be assigned to the intrinsic bandgap absorption of ZnO due to the electron transitions from the valence band to the conduction band. Powder XRD patterns confirmed the hexagonal wurtzite structure. Further, the SEM analysis also indicates the hexagonal rod shape structure of the ZnO nanoparticles. EDX spectra confirmed the chemical composition of the ZnO nanoparticles. In vitro antibacterial activity of ZnO nanoparticles were performed on three Gram (–ve) (*Escherichia coli*, *Klebsiella pneumoniae* and *Pseudomonas aeruginosa*) and one Gram (+ve) (*Staphylococcus aureus*) bacteria, in which the ZnO nanoparticles obtained by biological method showed excellent bactericidal activity.

71. **Kavitha et.al., (2017)** synthesized the ZnO nanoparticles using terpenoid (TAP) fractions isolated from *Andrographis paniculata* leaves. Subsequently, the ZnNO₃ (0.1 N) is treated with the isolated TAP fractions to biosynthesize zinc oxide nanoparticles (Zn-TAP NPs). This nanoparticle preparation has been confirmed by the color change from green to cloudy-white and the peak at 300 nm by UV–Visible spectra. FTIR analysis of Zn-TAP NPs showed the presence of functional group (i.e.) C=O which has further been confirmed by H¹-NMR studies. From SEM and XRD analysis, it has been found that the hexagonal nanorod particle is 20.23 nm in size and +17.6 mV of zeta potential. Hence, it can be easily absorbed by negatively charged cellular membranes to contribute for efficient intracellular distribution. Therefore, it is suggested that the synthesized Zn-TAP NPs are more suitable in drug delivery processes.

72. **Khajuria, et.al., (2017)** synthesized Zinc oxide Nanoparticles using leaf extract of *Viola canescens*. Synthesized nanoparticles were subjected to UV-Vis, XRD, FTIR and SEM analysis for further characterization. The average calculated size of ZnO nanoparticles was <26 nm and found to be hexagonal in structure recorded from XRD analysis. FTIR spectra showed the presence of —OH, C=C, C=O, and other groups which may be involved in reduction and capping of synthesized nanoparticles. Potential of ZnO nanoparticles as an anti-bacterial agent has been studied against two clinical isolates *Staphylococcus aureus* and *E. coli* and the zone of inhibition observed for both isolates clearly indicated their potential as an antimicrobial agent.

73. **Jeyabharathi, et.al., (2017)** synthesized zinc oxide nanoparticles (ZnONPs) using the extract of the plant, *Amaranthus caudatus*. ZnONPs were characterized by FTIR and SEM coupled with EDX. Among the various concentrations of ZnONPs administered, 10 mg/ml or more caused deformities and less survival rate. ZnONPs were found to influence the normal development of zebrafish embryos in a dose dependent manner. The ZnONPs were found to exhibit antibacterial activity; the activity was more towards Gram positive bacteria (*S. epidermidis*) than the Gramnegative bacteria (*E. aerogenes*). The low concentrations of ZnONPs could be used as a therapeutic agent for diabetes mellitus.

74. **Anand Raj and E. Jayalakshmy et.al., (2015)** synthesized the ZnO nanoparticles using the aqueous root extracts of *Zingiber officinale* (ginger). The root extracts were found to be rich in flavonoids which were confirmed by the flavonoid test thereby enhancing the biogenic synthesis of ZnO nanoparticles. The SEM with EDAX studies were used for characterization that provides the size and the elemental composition of the synthesized ZnO nanoparticles. The average size

of the nanoparticles was found to be 30-50 nm. The FTIR analysis played a pivotal role in displaying the important functional groups present in the ZnO nanoparticle, which showed that the sample had strong absorbance in the range of 1600 – 1450 cm⁻¹. Hence the biogenic synthesis of ZnO nanoparticles using *Zingiber officinale*, can be an alternative to chemical synthesis.

75. **Murali, et.al., (2017)** synthesized Zinc oxide nanoparticles (ZnO-NPs) for the first time from any of the species of *Ceropegia*. Presently, ZnO-NPs were synthesized from the leaf extract of *Ceropegia candelabrum* with zinc nitrate using a simple hydrothermal process. The synthesized ZnO-NPs showed an absorption peak at 320 nm which is one of the characteristic features of ZnO-NPs. The FT-IR characterization revealed a spectrum band at 551.93 cm⁻¹ corresponding to the functional group metal oxide. SEM images showed agglomeration of nanoparticles with a hexagonal shape. XRD results are in correlation with SEM images as the synthesized particles were of hexagonal wurtzite shape and the size of the particles was in the range of 12–35 nm calculated using Scherrer's formula. The elemental analysis using EDS confirmed high zinc content of 70.48% stating that the process of biosynthesis of nanoparticles was carried out in accordance. The biosynthesized ZnO-NPs offered significant antibacterial potential against *S. aureus*, *B. subtilis*, *E. coli* and *S. typhi*.

76. **Supraja, et.al., (2016)** synthesized zinc oxide nanoparticles using the stem bark extract of *Boswellia ovalifoliolata*, and evaluation of their antimicrobial efficacy. Stable ZnO nanoparticles were formed by treating 90 ml of 1 mM zinc nitrate aqueous solution with 10 ml of 10 % bark extract. The formation of *B. ovalifoliolata* bark-extract-mediated zinc oxide nanoparticles (BZnNPs) was confirmed by UV–visible spectroscopic analysis and recorded the localized surface plasmon resonance (LSPR) at 230 nm. FT-IR analysis revealed the functional groups present in the bark extract which are responsible for the reduction and stabilization of the BZnNPs. The morphology and crystalline phase of the

nanocrystals were determined by TEM. The hydrodynamic diameter (20.3 nm) and a positive zeta potential (4.8 mV) were measured using the dynamic light scattering technique. The antimicrobial activity of BZnNPs was evaluated (in vitro) against fungi, Gram-negative, and Gram-positive bacteria using disk diffusion method which were isolated from the scales formed in drinking water PVC pipelines.

77. **Manokari et.al., (2017)** synthesized the zinc oxide nanoparticles (ZnO NPs) from the aqueous extracts of aerial parts of *Hibiscus rosa-sinensis*. Zinc nitrate hexahydrate ($Zn(NO_3)_2 \cdot 6H_2O$) was used as a precursor and the extracts of leaves, stem segments and flower petals were used for the reduction of zinc oxide nanoparticles. The resulting reaction mixture with zinc colloids were characterized using UV-Visible spectrophotometric analysis. The absorbance peak was obtained at 300 nm, 291 nm and 293 nm for leaf, stem and flower petals respectively. This is an eco-friendly approach for quick scale up of ZnO nanoparticles from *H. rosa-sinensis* and it can be performed at room temperature.

79. **Vanathi et.al., (2014)** synthesized zinc oxide nanoparticles from aquatic weed by a green chemistry approach. The aim of this work is to synthesize zinc oxide nanoparticles from *Eichhornia crassipes* leaf extract by low cost technology as against the other available technique and eco-friendly method. Aqueous leaf extract acts as a reducing and capping agent during synthesis of nanoparticles. Formation of zinc oxide nanoparticles, optical properties, size and morphology has been analyzed by UV-vis spectrophotometer, XRD, SEM with EDX and TEM. SEM and TEM analysis show that zinc oxide nanoparticles were spherical in shape and average particle size was 32 ± 4 nm. Biological method for synthesis of zinc oxide nanoparticles using plant extracts has been suggested as a possible eco-friendly alternative to chemical and physical methods.

80. **Datta et.al., (2017)** synthesized zinc oxide nanoparticles from *Parthenium hysterophorus* leaf extracts. The Nanoparticles were extracted with the help of aqueous, methanolic and ethanolic solutions of P. hysterophorus leaves. Since a higher yield of nanoparticles was observed when synthesized using aqueous extract therefore these were used in further experiments. Synthesized nanoparticles were characterized using UV-Vis spectroscopy with maximum absorbance peak at 400 nm. SEM and TEM analysis revealed that the particles were spherical and cylindrical in shape with average particle size ranging from 16-45 nm. The chemical group association and elemental composition of nanoparticles was analyzed using FTIR and SEM-EDX. Green synthesized zinc oxide nanoparticles were evaluated for antimicrobial activities against Gram positive and Gram negative bacteria. Zinc nanoparticles exhibited maximum zone of inhibition against *Enterobacter aerogenes* (36 mm) while least activity was seen against *Staphylococcus aureus* and *Bacillus subtilis*.

MATERIALS

AND

METHODS

3.1 Materials

Zinc oxide nanoparticles were synthesized through the green synthesis method using plant extract. Zinc acetate dihydrate, plant extract, sodium hydroxide and ethanol were used for green synthesis. *Telosma cordata* leaves were collected from our university campus and confirmed with the help of the taxonomist of the Botany department of our university

3.2 Methodology:

The methodology pertaining to the title “A Green synthesis of Zinc oxide Nanoparticles using aqueous extract of *Telosma cordata* is presented in these chapter Zinc oxide nanoparticles were synthesised through two methods, the first one is through Chemical method and the second one is green synthesis using plant extract. Zinc oxide, starch and sodium hydroxide were used for chemical synthesis and zinc acetate dihydrate, Plant extract, sodium hydroxide and ethanol were used for green synthesis *Telosma cordata* leaves were collected from our university campus and confirmed the leaves with the help of botany department and they dried for one week.

3.2.1. Synthesis of ZnO nanoparticles

Chemical method

20ml of 0.1 M zinc oxide was taken in a conical flask. To the solution added 0.1% of starch solution (prepared by dissolving 0.01g of starch in 10ml of water). The above solution was stirred for 1hr on a magnetic stirrer, then added 2ml of 0.2M NaOH and kept in incubation for 24 hrs.

Green synthesis

Green synthesis of zinc oxide nanoparticles were done with *Telosma cordata* leaves extract.

Preparation of leaf extract

Fresh leaves of *Telosma Cordata* were thoroughly cleaned with running tap water to remove debris and other contaminants, followed by distilled water and air dried at room temperature. Leaves were finely chopped into small pieces. The aqueous extract of sample was prepared by boiling the freshly collected cut leaves (10g), with 100 ml of distilled water, at 60°C for about 20 minutes, until the colour of the aqueous solution changes from watery to light brown. Then the extract was cooled to room temperature and filtered using Whatman filter paper. The extract was stored in a refrigerator in order to be used for further experiments

Phytochemical screening

Phytochemical examinations were carried out for all the extracts as per standard methods (**Prashant Tiwari *et al.*, Jan-March 2011**).

Detection of alkaloids: Extracts were dissolved individually in dilute Hydrochloric acid and filtered.

Mayer's Test: Filtrates were treated with Mayer's reagent (Potassium Mercuric Iodide). Formation of a yellow coloured precipitate indicates the presence of alkaloids.

2.Wagner's Test: Filtrates were treated with Wagner's reagent (Iodine in Potassium Iodide) Formation of brown/reddish precipitate indicates the presence of alkaloids.

Dragendroff's Test: Filtrates were treated with Drangendroff's reagent (Solution of Potassium Bismuth Iodide). Formation of red precipitate indicates the presence of alkaloids.

Hager's Test: Filtrates were treated with Hager's reagent (Saturated picric acid solution) Presence of alkaloids confirmed by the formation of yellow coloured precipitate.

Detection of carbohydrates: Extracts were dissolved individually in 5 ml distilled water and filtered. The filtrates were used to test for the presence of carbohydrates.

Molisch's Test: Filtrates were treated with 2 drops of alcoholic α -naphthol solution in a test tube. Formation of the violet ring at the junction indicates the presence of Carbohydrates.

Benedict's Test: Filtrates were treated with Benedict's reagent and heated gently. Orange red precipitate indicates the presence of reducing sugars.

Fehling's Test: Filtrates were hydrolysed with dil. HCl, neutralized with alkali and heated with Fehling's A & B solutions. Formation of red precipitate indicates the presence of reducing sugars.

Detection of glycosides: Extracts were hydrolysed with dil. HCl, and then subjected to a test for glycosides.

Modified Borntrager's Test: Extracts were treated with Ferric Chloride solution and immersed in boiling water for about 5 minutes. The mixture was cooled and extracted with equal volumes of benzene. The benzene layer was separated and treated with ammonia solution. Formation of rose pink colour in the ammoniacal layer indicates the presence of anthranol glycosides.

Legal's Test: Extracts were treated with sodium nitroprusside in pyridine and sodium hydroxide. Formation of pink to blood red colour indicates the presence of cardiac glycosides.

Detection of saponins

Froth Test: Extracts were diluted with distilled water to 20ml and this was shaken in a graduated cylinder for 15 minutes. Formation of 1 cm layer of foam indicates the presence of saponins.

Foam Test: 0.5 gm of extract was shaken with 2 ml of water. If foam produced persists for ten minutes it indicates the presence of saponins.

Detection of phytosterols

Salkowski's Test: Extracts were treated with chloroform and filtered. The filtrates were treated with few drops of Conc. Sulphuric acid, shaken and allowed to stand. Appearance of golden yellow colour indicates the presence of triterpenes.

3.Libermann Burchard's test: Extracts were treated with chloroform and filtered. The filtrates were treated with few drops of acetic anhydride, boiled and cooled. Conc. Sulphuric acid was added. Formation of the brown ring at the junction indicates the presence of phytosterols.

Detection of phenols

Ferric Chloride Test: Extracts were treated with 3-4 drops of ferric chloride solution. Formation of bluish black colour indicates the presence of phenols.

Detection of tannins

Gelatin Test: To the extract, 1% gelatin solution containing sodium chloride was added. Formation of white precipitate indicates the presence of tannins.

Detection of flavonoids

Alkaline Reagent Test: Extracts were treated with few drops of sodium hydroxide solution. Formation of intense yellow colour, which becomes colourless on addition of dilute acid, indicates the presence of flavonoids.

Lead acetate Test: Extracts were treated with few drops of lead acetate solution. Formation of yellow colour precipitate indicates the presence of flavonoids.

Detection of proteins and amino acids

Xanthoproteic Test: The extracts were treated with few drops of conc. Nitric acid. Formation of yellow colour indicates the presence of proteins.

Ninhydrin Test: To the extract, 0.25% w/v ninhydrin reagent was added and boiled for few minutes. Formation of blue colour indicates the presence of amino acid ZnO Synthesis from plant extract

For the synthesis of ZnO nanoparticles, 50ml of 0.5M zinc acetate dihydrate solution was prepared using distilled water. 1ml of aqueous leaf extract was introduced into the above solution After 10 minutes stirring. In order to maintain the pH 12 NaOH solution was added drop by drop, which resulted in a pale white aqueous solution This was then placed in a magnetic stirrer for 2 hrs. The pale white precipitate was then taken out and washed over and over with distilled water and then with ethanol to remove impurities.

Then a pale white powder of ZnO nanoparticles was obtained after drying in the oven. (Snehal yedurkar *et al.*, 2016.)

3.2.3 Characterization of Nanoparticles

Characterization of nanoparticles was done by different methods. UV-visible spectral analysis was used to analyse the absorbance. Fourier transform infrared spectroscopy (FT-IR) gives. Specific signals for NPs .shape of the nanoparticle were characterized by scanning electron microscopy, thermo gravimetric analysis, LASER analysis is used to topography and roughness of nanoparticles.

UV-visible analysis

UV-visible spectroscopy is usually conducted to confirm the synthesis of ZnO NPs Peaks. Which studied in the range of 200-400 nm. Different peaks are obtained in this range. Absorbance also obtained through this analysis. Conducting electrons start oscillating at a certain wavelength range due to surface Plasmon resonance. (Santhosh Kumar *et al.*, 2017)

FT-IR analysis

Specific signals obtained by IR spectroscopy according to the vibrations of the molecule. FT-IR spectra and functional groups involved in ZnO NPs synthesis illustrated peaks in the range of 500-4000cm⁻¹..The sample pellet was placed into the sample holder and FT-IR spectra were recorded in FT-IR spectroscopy.

SEM Analysis

SEM analysis is used to visualize the shape and size of nanoparticles. Scanning electron microscopy was adjusted in different magnifications and used to determine the shape of ZnONPs. SEM images in different magnification ranges can be evaluated. (Santhosh Kumar *et al.*, 2017). SEM image was usually used to study the morphology of synthesised nanoparticles (Kalpana handore. *et al.*, 2014)

3D Optical Profilometry

LASER and AFM analyses have given us insight about the topography, roughness of nanoparticles. LASER imaging was conducted in different magnification range images clearly demonstrating smooth nanoparticles with capping of phyto- chemicals over the surface of nanoparticles (Santhosh Kumar j. *et al.*, 2017). It is commonly used for obtaining colloidal solutions of nanoparticles. This analysis also helps in determining morphology and surface studies.

Thermo gravimetric analysis

TGA is a method of thermal analysis in which changes in physical and chemical properties of materials are measured as a function of increasing temperature or as a function of time with constant temperature. It is a temperature based study.

Anti-microbial activity studies

Agar disc diffusion method is used for antimicrobial studies and by this technique we can say that ZnO nanoparticles are how much effective the microbes like E-coli, s-aureus. These NPs exhibit antifungal, anticorrosive, antibacterial properties due to increased specific surface area, reduced particle size, enhanced particle surface reactivity and abrasive surface texture or surface defect ZnO NPs have recently shown to provide effective pathogen growth control as they have lower toxicity as well as positive impact on soil fertility. The chemically synthesized ZnO NPs have been found to be convincing antibacterial agents because they have the ability to absorb UV radiation and the inhibition efficiency of microbes studied. The cultures were stocked at 4°C after subculturing incubation

of 24hrs at 37°C in incubator. Mueller hinton agar were prepared and sterilized at 121°C for 15 minutes the antibacterial assays were carried out the agar well-diffusion method (**Jesteena *et al.*, 2017**) Mueller Hinton agar plate were prepared and after solidification 60µl of culture were poured and spread with sterile cotton swab and kept for drying 2-3 minutes Wells were made with cork borer in the diameter of 5mm and added the sample separately around 50µl I each well. All the plates were incubated at 37°C For 24hrs. The diameters of the inhibition zone produced by the extract were measured in mm after the incubation period.

RESULTS

&

DISCUSSION

4. RESULT AND DISCUSSION

The present investigation entitled “Ecofriendly Synthesized of Zinc oxide nanoparticles by *Telosma cordata* leaves” deals with the synthesis of zinc oxide nanoparticles from *Telosma cordata* leaves extract characterization studies were carried out with the synthesized nanoparticles. Antibacterial activity of the zinc oxide nanoparticles was also studied using four different bacterial

4.1. Qualitative Phytochemical Analysis

The Phytochemical analysis of the plant extract of *Telosma cordata* leaves is shown in table 4.1.1. The analysis revealed the presence of several phytochemical such as flavonoids, alkaloids , saponins and tannins . The result + sign represents and sign represents the absence of compound.

S.No	Chemical constituent	Phytochemicals test	Result
1	Alkaloids	Dragendorff's test	+
2	Glycoside	Legal's test	-
3	Phenolic test	Ferric chloride test	+
4	Tannins	Gelatin test	-
5	Saponins	Foam test	+
6	Carbohydrates	Fehling's test	-
7	Flavonoids	Alkaline reagent test	+
8	Proteins	Xanthoproteic test	-
9	Amino acid	Ninhydrin test	-

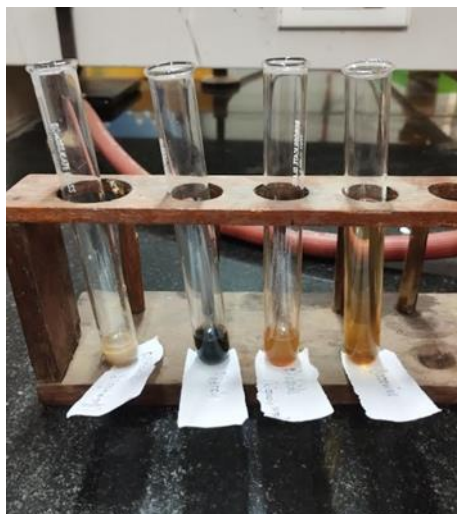
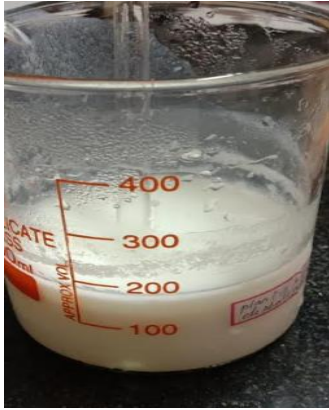


Fig 4.1.1 Phytochemical Screening

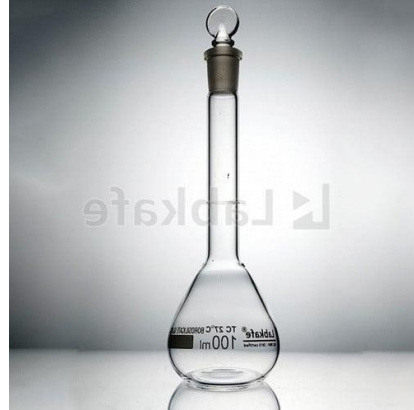
ZnO Synthesis from plant extract

For the synthesis of ZnO nanoparticles, 50ml of 0.5M Zinc acetate dihydrate solution was prepared using distilled water. 1ml aqueous leaf extract was introduced into the above solution. After 10 minutes stirring. In order to maintain a pH of 12, NaOH solution was added drop by drop, which resulted in a pale white aqueous solution. This was then placed in a magnetic stirrer for 2 hrs. The pale white precipitate was then taken out and washed over and over with distilled water and then with ethanol to remove impurities. Then a pale white powder of ZnO nanoparticles was obtained after drying in the oven.



Plant extract

+



50ml of 0.5M Zinc oxide acetate dihydrate



Stirring for 10 mins



Stirring for 2 hrs



Product

Fig 4.1.2 Biosynthesis of ZnO nanoparticles (ZnO NPs) using plant extract

Characterization

The Characterization of Zinc Oxide Nano Particles was carried out using the methods

- UV-Visible analysis
- FT-IR analysis
- 3D Optical Profilometry
- SEM
- EDAX
- XRD
- TGA analysis
- Antibacterial activity

4.2 UV - Visible Spectroscopy

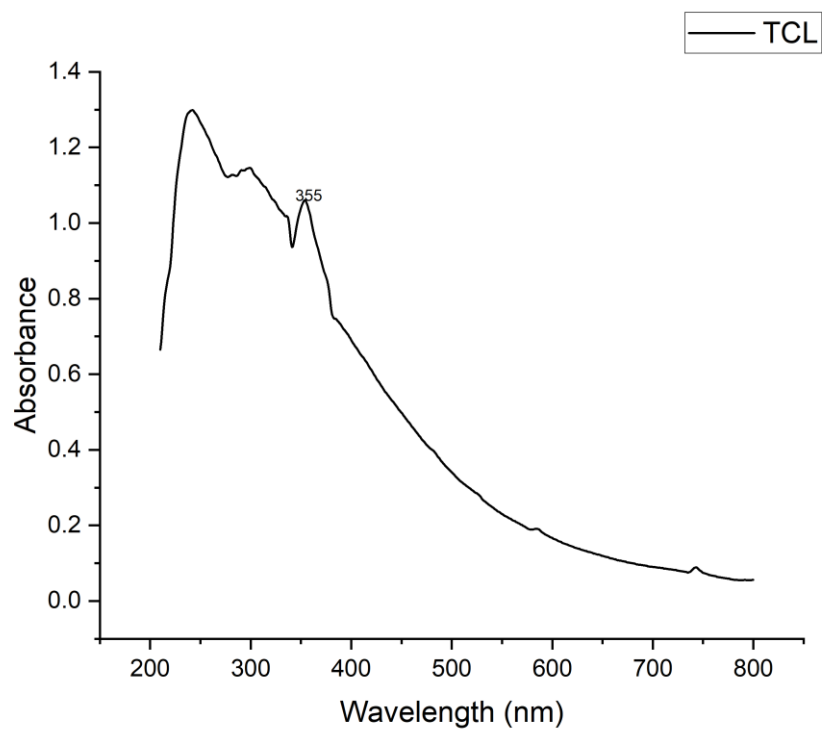


Fig 4.2.1 UV-Visible is spectrum of green synthesized ZnO NPs

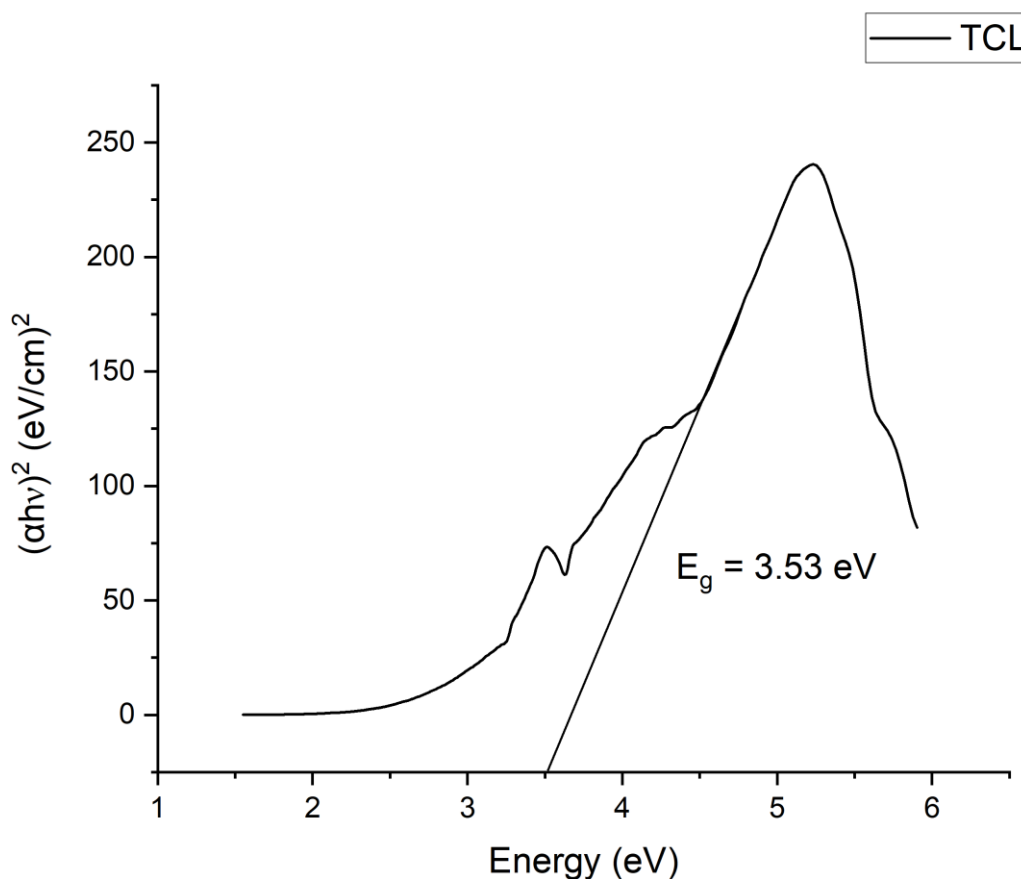


Fig 4.2.2 Band gap energy of green synthesized ZnO NPs

The absorption spectra of Zinc Oxide Nanoparticles were recorded using a double beam UV-Visible spectrophotometer. For chemically synthesized Zinc oxide nanoparticles, It analysed by measuring the UV-visible spectrum which clearly indicated that the intense characteristic absorption peaks were between 200-800nm. The absorption maximum was obtained at 355nm which confirms the synthesis of zinc oxide nanoparticles whereas the geen synthesis of zinc oxide nanoparticles were synthesized using *Telosma cordata* leaf extract which was recorded at different wavelength is the range of 200-800nm. The spectrum showed

the absorbance peaks at 301nm which is corresponding to the characteristics band of ZnO.

4.3 FT-IR SPECTROSCOPY

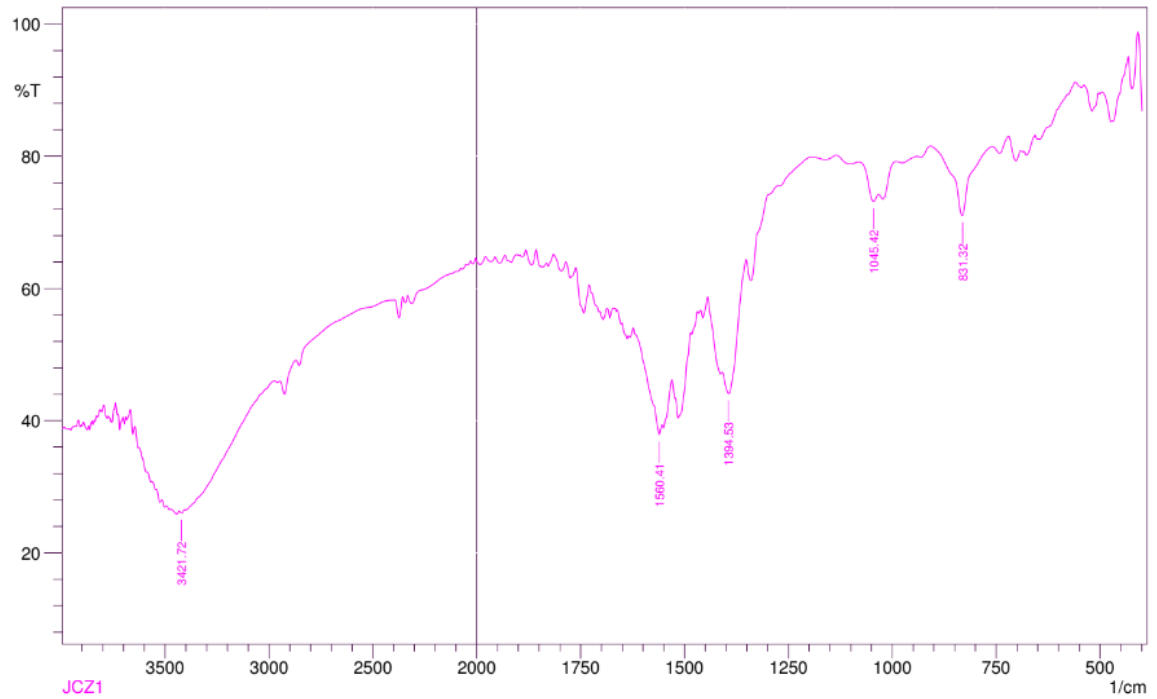


Fig 4.3.1 FT-IR spectrum of green synthesized ZnO NPs

Vibrational frequency cm^{-1}	Functional group	Reference
3422	O-H Stretching	Vijayakumar <i>et.al.</i> ,2016
1561	C=C Stretching	Bala <i>et.al.</i> ,2016
1054	C-O Stretching	Ramesh <i>et.al.</i> ,2021
831	C-H Bending	Vijayakumar <i>et.al.</i> ,2016

Table 4.3.2 Spectral range and functional group of green synthesized ZnO NPs.

FTIR Spectroscopy is used to identify the plant extract present in the synthesized nanoparticles. The analysis was done at a frequency range of 4000-400 cm^{-1} at room temperature. Some intense peaks in the recorded spectra were observed, which can be assigned to the presence of some functional groups such as -O-H,-C=C, -C-O , Stretching vibrations , -C-H, Bending , which formed a bio-capped layer aroundthe ZnO NPs. The sharp peak observed at 1561 cm^{-1} , 831 cm^{-1} confirmed the formation of ZnONPs (Nagaraju *et al.*, 2017). The peaks observed at 831 cm^{-1} can be assigned to C-H bending. A broad peak at 3421 cm^{-1} corresponds to the presence of O-H stretching vibration (Chinnammal Janaki *et al.*, 2015). The formation of the ZnO NPs confirms that the aqueous extract of *Telosma cordata* plant can act as a natural stabilizer or capping agent to produce the small particles . It may be causes by the presence of some bioactive compounds in the plant extract

4.4 X-Ray Diffraction

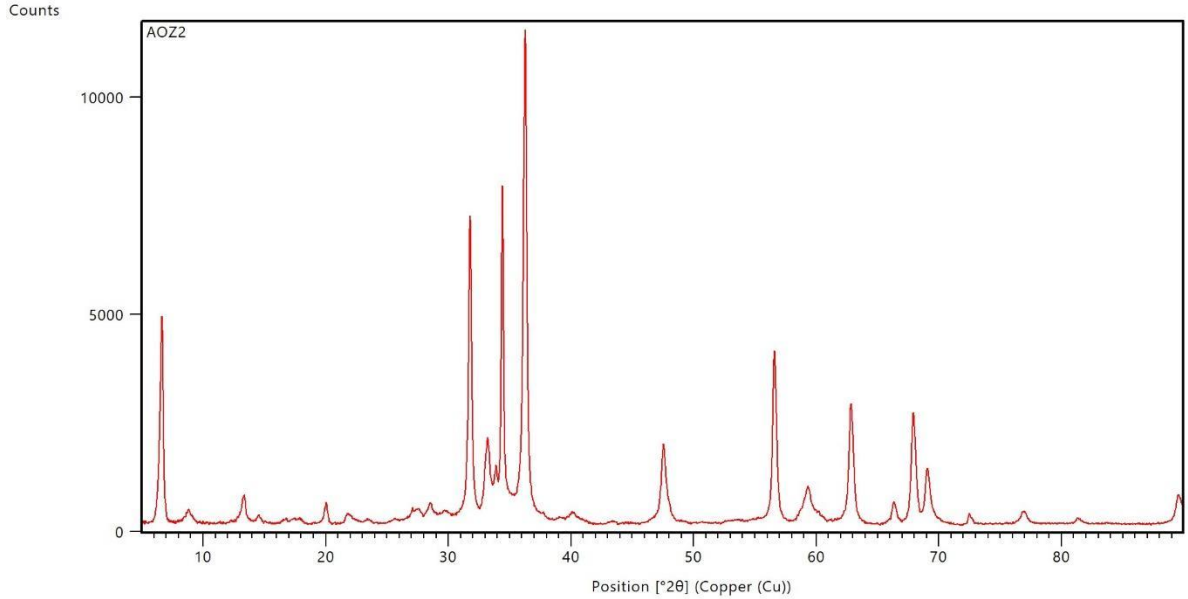


Fig 4.4.1 XRD image of green synthesized ZnO NPs

The XRD pattern of zinc oxide nanoparticles synthesized by the plant-mediated approach. The peak located at 9.65, 31.5, 34.1, 36.1, 47.9, 57.8, 59.2, 66.1, 68.25, 69.1 (**Awwad *et.al.*,2013**) are corresponding to planes. Thus the results indicated that the XRD spectrum has sharp peak and narrow diffraction peaks indicating that the synthesized nanoparticles are pure and crystalline peak. Scherret equation were used to measure the average crystalline size $D=K\lambda/(\beta,\cos\Theta)$ where D is the average crystalline size in Å, λ is the wavelength of X-ray

(1.5406 Å) Cu α radiation, K is the shape factor (0.9) β is the full width half wave maximum (FWHM) of the biosynthesized nanoparticles and Θ is the diffraction. The crystallite size of *Telosma cordata* associated zinc oxide nanoparticles mediated zinc oxide nanoparticles were found to be 13.3 nm respect. (**K. Manjunath *et.al.*,2016**)

S.No	Degree (Θ)	FWHM(β)	Crystallite size (D)
1.	6.54	0.33	24.67
2.	8.43	0.78	10.67
3.	12.66	1.07	7.78
4.	29.91	4.40	1.95
5.	31.70	0.32	26.50
6.	33.00	0.53	16.11
7.	34.14	1.31	6.59
8.	36.19	0.32	27.12
9.	59.21	1.44	6.62
10.	36.13	1.71	5.10
Average crystallite size = 13.31nm			

Table 4.4.2 Structure and geometric parameters of green synthesized ZnO NPs

4.5 SEM

The surface morphology of the resulting powder is examined using scanning electron microscope. From the image it is evident that the morphology of zinc oxide nanoparticles is spherical is spherical shaped and well distributed with aggregation observed which is very similar to earlier studies. The surface energy of ZnONPs that usually occurs when synthesis is carried out in aqueous medium and also possibly due to densification resulting in narrow space between particles .
(**J.P.Shabaaz Begum *et.al.*,2017**)

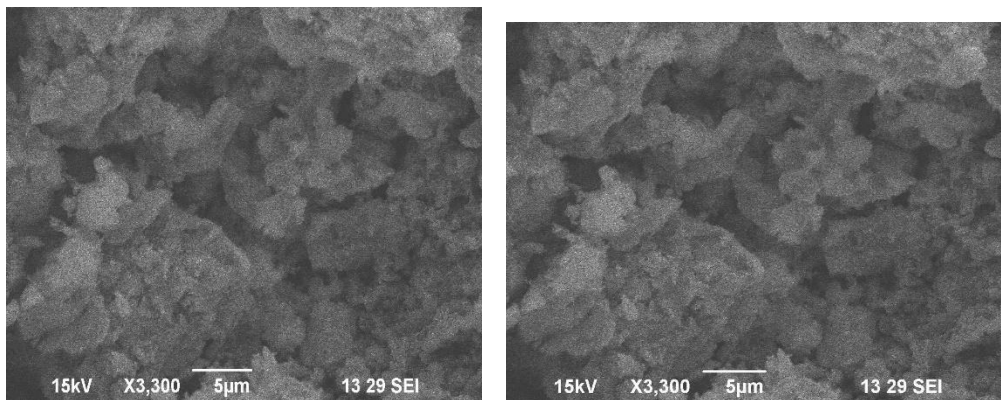


Fig 4.5.1 SEM images of green synthesis ZnO NPs

4.6 EDX:

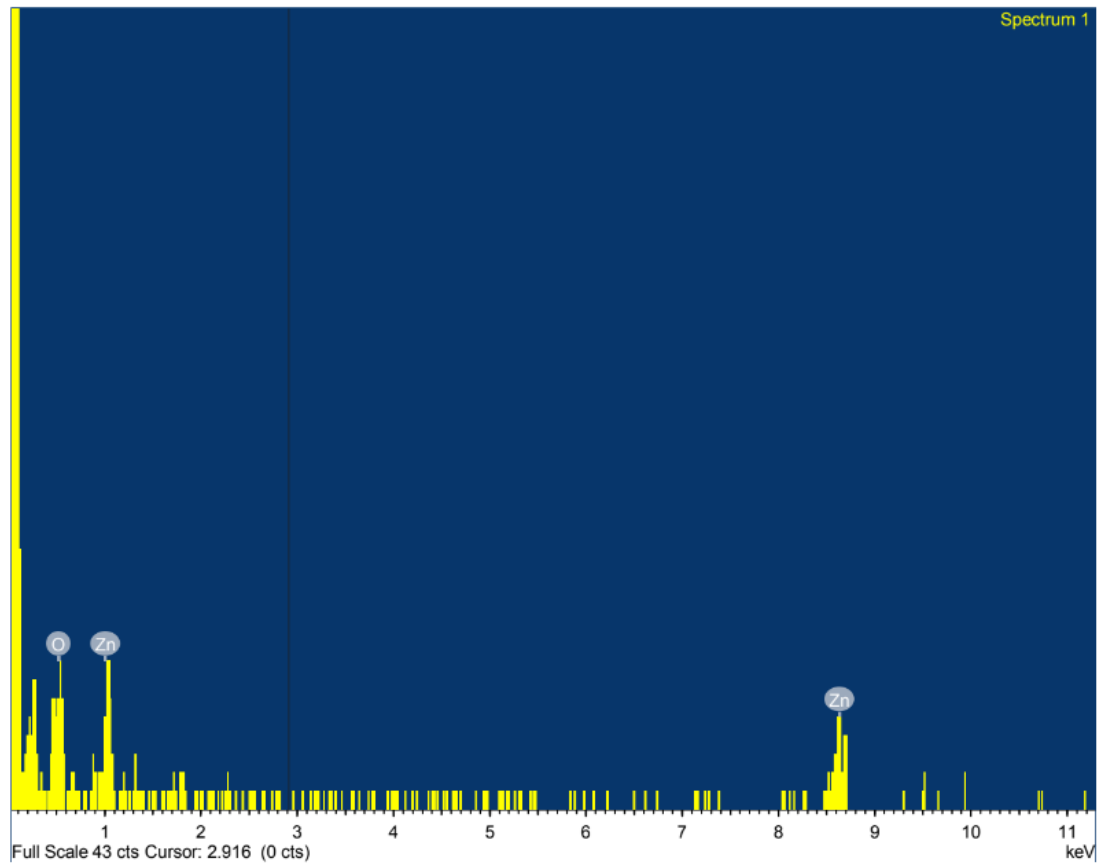


Fig4.6.1 EDX image of green synthesized ZnONPs

The EDX spectrum show only the peaks of zinc oxide nanoparticles confirms the presence of the element zinc and oxygen signals. This research revealed that the peaks corresponded to the manufactured nanoparticle's optical absorption

Element	Weight%	Atomic%
O	0.05	59.34
Zn	0.05	40.66

Table 4.6.1 EDX value of green synthesized ZnO NPs

4.7 Antibacterial activity

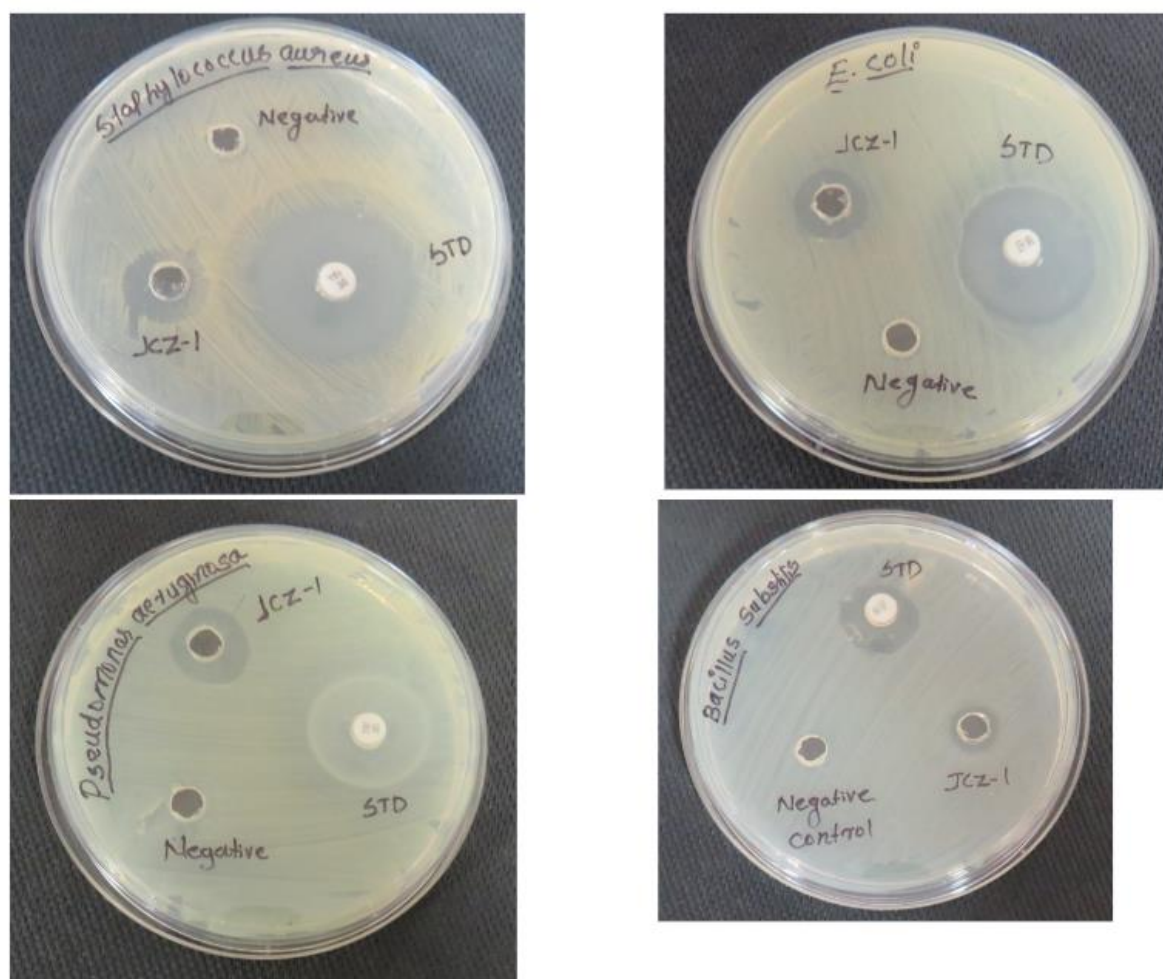


Fig 4.7.1 Antibacterial activity of Inhibition zone of green synthesized ZnO

The green synthesized ZnO NPs against human pathogenic bacterial strains as an antibacterial agent. MIC of the microbicidal compound against bacterial is the minimal value to constrain the viable bacterial growth .(**Pratibha et.al.**) In contrast , MBC is the lowermost concentration of the antibiotic compound that is fatal to the bacteria in the micro broth dilution technique as shown in fig 4.41 MIC and MBC values of all green synthesized ZnO NPs against pathogenic bacterial are tabulated in table 2. Phytonanofabricated ZnO NPs showd noteworthy antibacterial activity against *Staphylococcus aureus* , *Bacillus cereus* , *Pseudomonas aeruginosa* and *Escherichia coli* with discretre modifications in the susceptability to ZnO NPs(**Shabaaz Begum et.al.**)

Samples	Zone of Inhibition (mm)			
	<i>Staphylococcus aureus</i>	<i>Bacillus subtilis</i>	<i>Escherichia coli</i>	<i>pseudomonas aeruginosa</i>
Standard*	29mm	12mm	26mm	25mm
Negative control	0mm	0mm	0mm	0mm
JCZ-1	14mm	11mm	15mm	16mm

Table 4.7.1 Zone of Inhibition

4.8 TGA

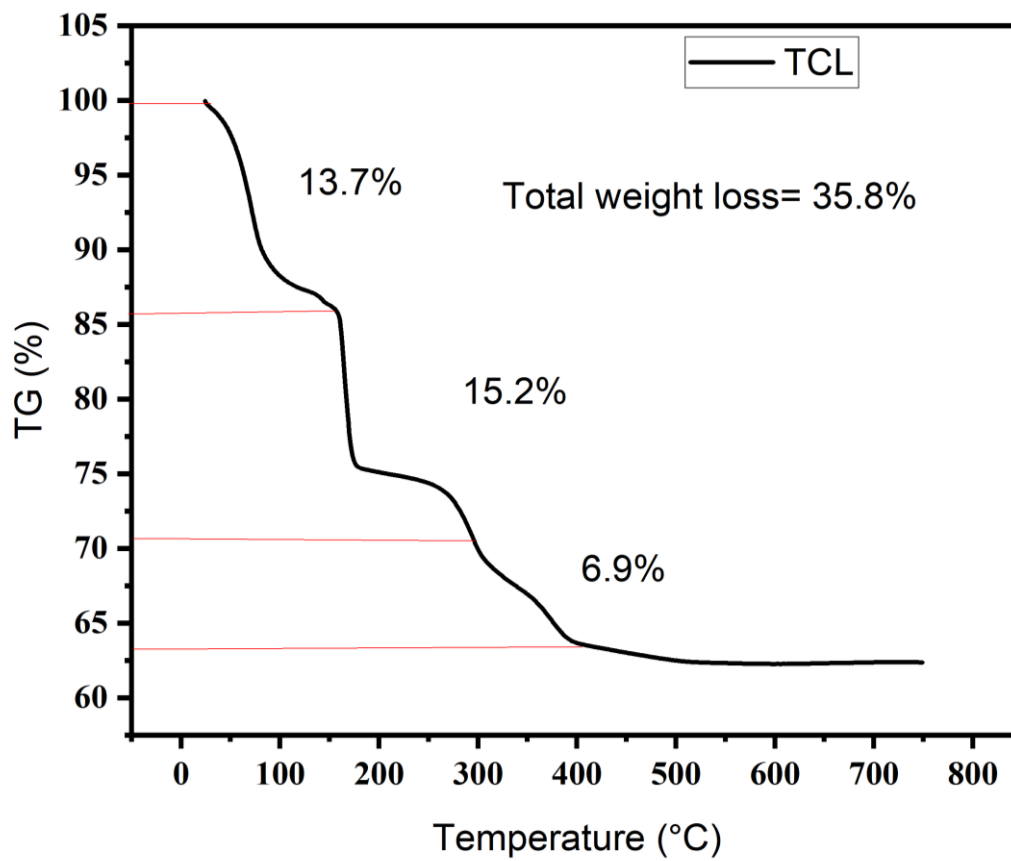


Fig 4.8.1 TG image of green synthesized ZnO NPs

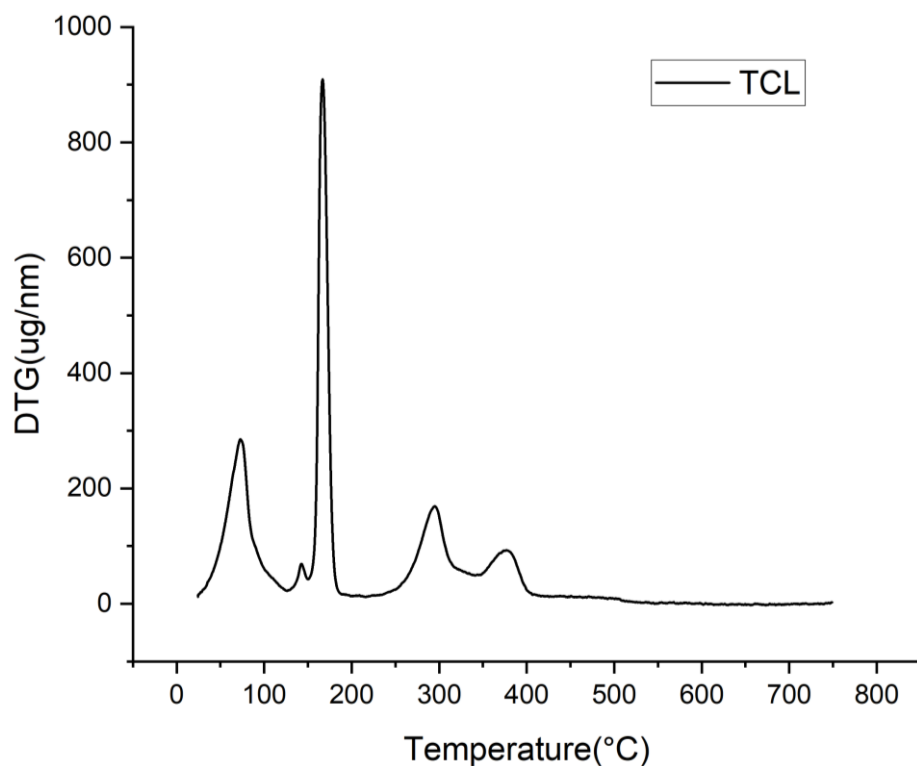


Fig 4.8.2 Derivative TG curve of green synthesized ZnO NPs

TGA and differential thermal analysis indicate the thermal stability of nanoparticles. The temperature scale for the measurement was taken from 30 to 800°C. The thermal gravimetric analysis of ZnO NPs was performed on EXSTAR/6300 Thermogravimetric Analyser. TG curve of the synthesized ZnO NPs is shown in Fig----- and its derivative curve is shown in Fig---. The synthesized nanoparticles shown that the weight decreased upto 800°C. The total weight decrease was 8% approximately. The weight loss at 100 to 200°C may be due to thermal desorption of water and carbon dioxide from the surface of ZnO particles TG curve of ZnO formed at a temperature between 200°C and 600°C might indicate the formation of nanoparticles ZnO

(Prashanth *et.al.*,2015). Weight loss between 600 to 800°C may be because of thermal decomposition of plant bioorganic molecules present on the surface of ZnO NPs. As reported before, at temperature above 800°C there may be no weight loss in the TGA curve indicating that the ZnO NPs were stable within this temperature range (Padalia *et.al.*,2017)

4.9 3-D Optical Profilometer

Optical profilometer studies give us insight about the topography, roughness of nanoparticles. Images clearly demonstrate the nanoparticles with capping of phytochemicals over the surface of nanoparticles (Santhoshkumar *et.al.*,)

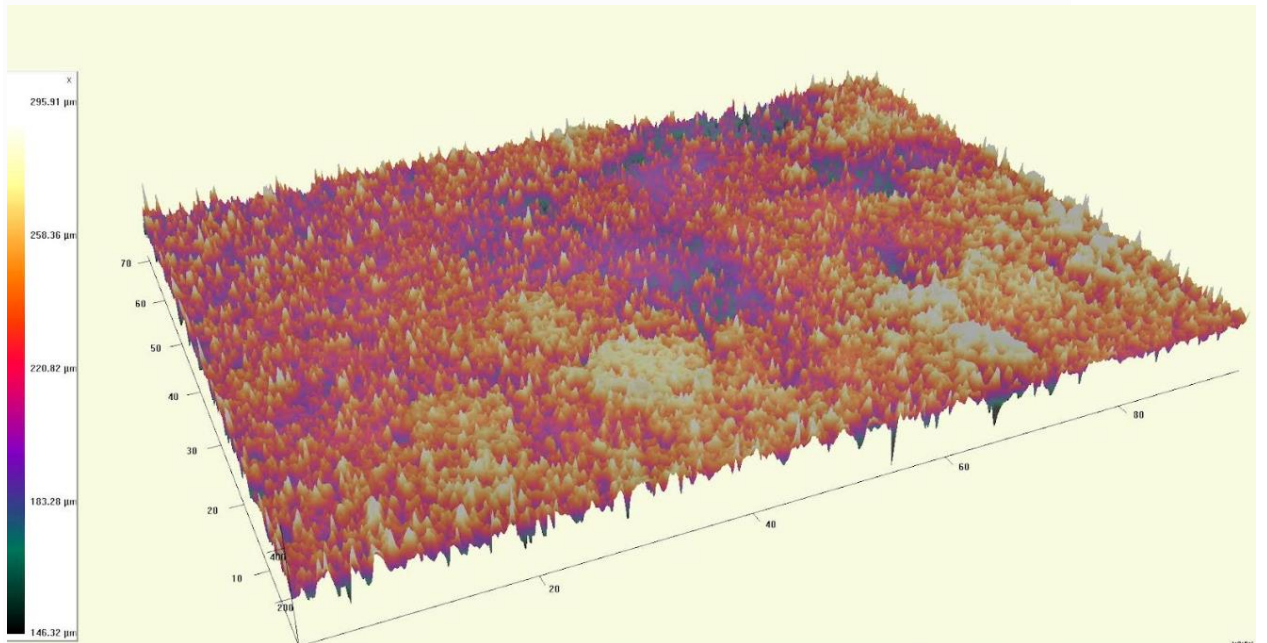


Fig 4.9.1 3D Optical Profilometer image of green synthesized ZnO NPs

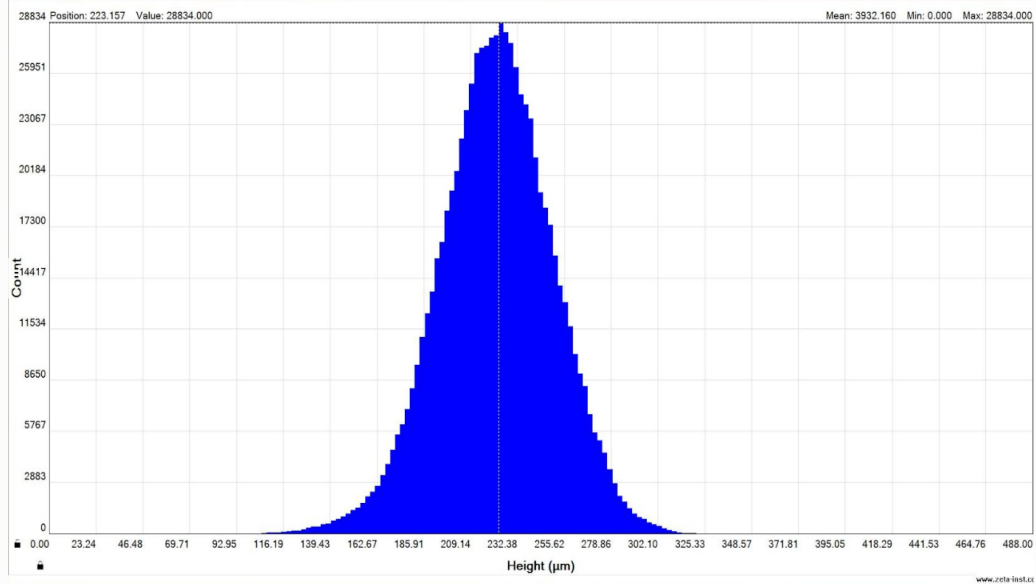


Fig 4.9.2 Histogram image of green synthesized of ZnO NPs

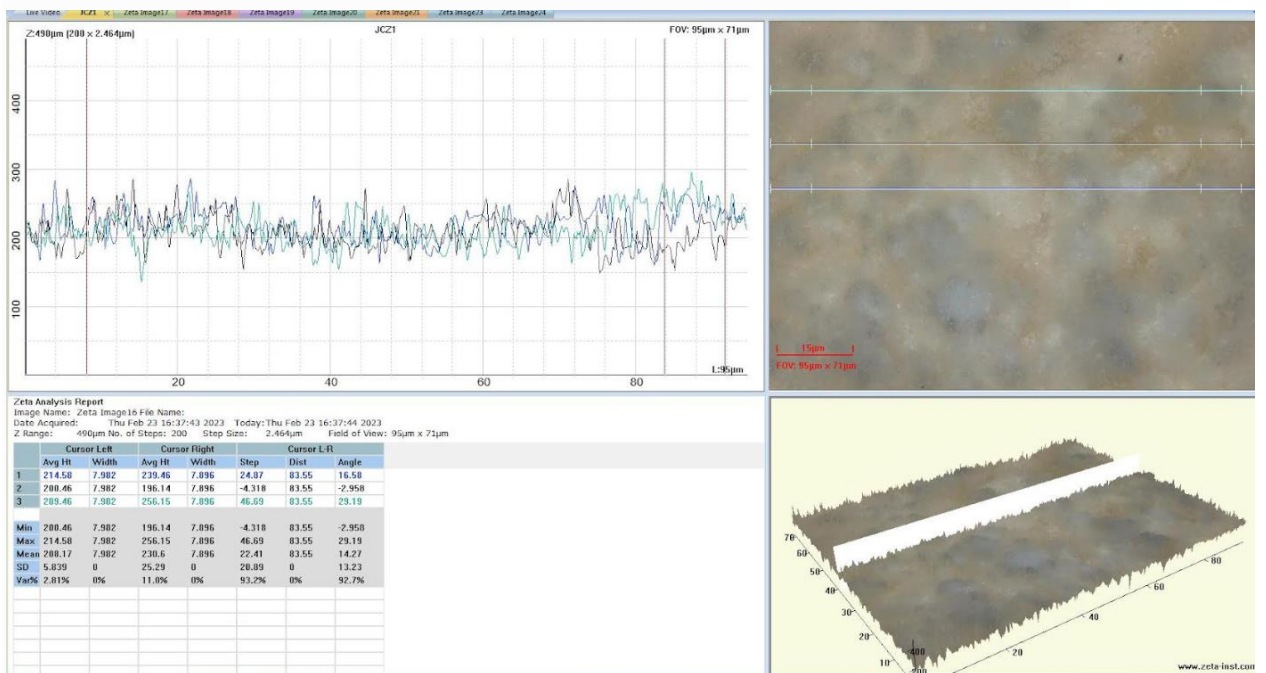


Fig 4.9.3 3D Optical Profilometer of cross section

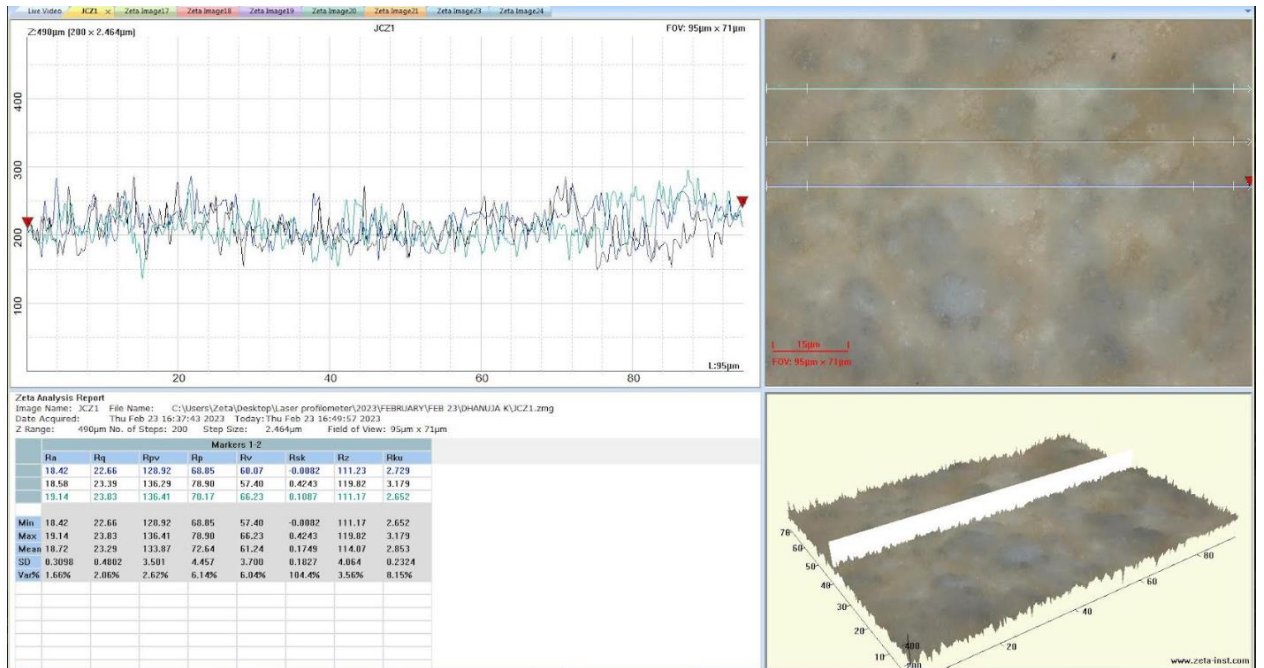


Fig 4.9.4 3D Optical Profilometer of roughness

Sample	Ra	Rq
Green synthesis of ZnO NPs	19.14	23.03

Table 4.9.5 Ra and Rq value of green synthesized ZnO NPs

SUMMARY

&

CONCLUSION

5. SUMMARY AND CONCLUSION

This is the first report on the photosynthesis of ZnO NPs from various volumes of a leaf extract *Telosma cordata*, which was used as a reducing agent. The synthesized nanoparticles were characterized and confirmed for the formation of plant extract in zinc oxide nanoparticles. The structural, morphological and antibacterial activities of prepared nanoparticles were characterized by FTIR Spectroscopy, XRD, 3D Optical Profilometry and well diffusion method. The obtained results from the present study revealed that *Telosma cordata* plant extract several natural bioactive compounds which those could be effectively utilized in the nanoparticles synthesis. XRD pattern has revealed the structure with crystalline size of 13.31 nm for zinc oxide

The nanoparticles were characterized by using XRD, FT-IR, SEM, EDX, UV, TGA, 3D Optical Profilometer and Antibacterial. The FT-IR analysis revealed the presence of biomolecules present in the plant extract that may have played a vital part in the formation of zinc oxide nanoparticles. SEM images clearly showed that the synthesised zinc oxide nanoparticles from *Telosma cordata* are needed regarding the application of these in the fields of water remediation and also about the photocatalytic properties.

BIBLIOGRAPHY

6. BIBLIOGRAPHY

1. Ganesh, P., Kumar, K. S., Geetha, D. E., & Kumar, T. S. (2013). Performance evaluation of cloud service with hadoop for twitter data. *Indonesian Journal of Electrical Engineering and Computer Science*, 13(1), 392-404.
2. Vidya, C., Hiremath, S., Chandraprabha, M. N., Antonyraj, M. L., Gopal, I. V., Jain, A., & Bansal, K. (2013). Green synthesis of ZnO nanoparticles by *Calotropis gigantea*. *Int J Curr Eng Technol*, 1(1), 118-120.
3. Samat, N. A., & Nor, R. M. (2013). Sol-gel synthesis of zinc oxide nanoparticles using *Citrus aurantifolia* extracts. *Ceramics International*, 39, S545-S548.
4. Vishwakarma, K. (2013). *Green synthesis of ZnO nanoparticles using *Abrus precatorius* seeds extract and their characterization* (Doctoral dissertation).
5. Zikalala, N. E., Azizi, S., Zikalala, S. A., Kamika, I., Maaza, M., Zinatizadeh, A. A., ... & Kaviyarasu, K. (2022). An Evaluation of the Biocatalyst for the Synthesis and Application of Zinc Oxide Nanoparticles for Water Remediation—A Review. *Catalysts*, 12(11), 1442.
6. Rajiv, P., Rajeshwari, S., & Venckatesh, R. (2013). Bio-Fabrication of zinc oxide nanoparticles using leaf extract of *Parthenium hysterophorus* L. and its size-dependent antifungal activity against plant fungal pathogens. *Spectrochimica Acta Part A: Molecular and Biomolecular Spectroscopy*, 112, 384-387.
7. Li, X., Wang, Q., Zhao, Y., Wu, W., Chen, J., & Meng, H. (2013). Green synthesis and photo-catalytic performances for ZnO-reduced graphene oxide nanocomposites. *Journal of colloid and interface science*, 411, 69-75.
8. 2014; 2013. Jansi Rani B. Praveen Kumar M. Ravi G. Ravichandran S. Guduru R. Yuvakkumar R. Saravanakumar B. Ramachandran S.P. Ganesh V. Sakunthala A.
9. Senthilkumar, S. R., & Sivakumar, T. (2014). Green tea (*Camellia sinensis*) mediated synthesis of zinc oxide (ZnO) nanoparticles and studies on their antimicrobial activities. *Int. J. Pharm. Pharm. Sci*, 6(6), 461-465.
10. Salam, H. A., Sivaraj, R., & Venckatesh, R. (2014). Green synthesis and characterization of zinc oxide nanoparticles from *Ocimum basilicum* L. var. *purpurascens* Benth.-Lamiaceae leaf extract. *Materials letters*, 131, 16-18.

11. Devi, R. S., & Gayathri, R. (2014). Green synthesis of zinc oxide nanoparticles by using *Hibiscus rosa-sinensis*. *Int. J. Curr. Eng. Technol*, 4(4), 2444-2446.
12. Bala, N., Dey, A., Das, S., Basu, R., & Nandy, P. (2014). Effect of hydroxyapatite nanorod on chickpea (*Cicer arietinum*) plant growth and its possible use as nanofertilizer. *Iranian Journal of Plant Physiology*, 4(3), 1061-1069.
13. Kundu, D., Hazra, C., Chatterjee, A., Chaudhari, A., & Mishra, S. (2014). Extracellular biosynthesis of zinc oxide nanoparticles using *Rhodococcus pyridinivorans* NT2: multifunctional textile finishing, biosafety evaluation and in vitro drug delivery in colon carcinoma. *Journal of photochemistry and photobiology B: Biology*, 140, 194-204.
14. Asadi, M., Kumar, B., Behranginia, A., Rosen, B. A., Baskin, A., Reppin, N., ... & Salehi-Khojin, A. (2014). Robust carbon dioxide reduction on molybdenum disulphide edges. *Nature communications*, 5(1), 4470.
15. Vanathi, P., Rajiv, P., Narendhran, S., Rajeshwari, S., Rahman, P. K., & Venckatesh, R. (2014). Biosynthesis and characterization of phyto mediated zinc oxide nanoparticles: a green chemistry approach. *Materials Letters*, 134, 13-15.
16. Davar, F., Majedi, A., & Mirzaei, A. (2015). Green synthesis of ZnO nanoparticles and its application in the degradation of some dyes. *Journal of the American Ceramic Society*, 98(6), 1739-1746.
17. Kalaiselvi, A., Roopan, S. M., Madhumitha, G., Ramalingam, C., & Elango, G. (2015). Synthesis and characterization of palladium nanoparticles using *Catharanthus roseus* leaf extract and its application in the photo-catalytic degradation. *Spectrochimica Acta Part A: Molecular and Biomolecular Spectroscopy*, 135, 116-119.
18. Sundrarajan, M., Ambika, S., & Bharathi, K. (2015). Plant-extract mediated synthesis of ZnO nanoparticles using *Pongamia pinnata* and their activity against pathogenic bacteria. *Advanced powder technology*, 26(5), 1294-1299.
19. Thema, F. T., Manikandan, E., Dhlamini, M. S., & Maaza, M. J. M. L. (2015). Green synthesis of ZnO nanoparticles via *Agathosma betulina* natural extract. *Materials Letters*, 161, 124-127.

20. Naika, H. R., Lingaraju, K., Manjunath, K., Kumar, D., Nagaraju, G., Suresh, D., & Nagabhushana, H. (2015). Green synthesis of CuO nanoparticles using *Gloriosa superba* L. extract and their antibacterial activity. *Journal of Taibah University for Science*, 9(1), 7-12.
21. Sundrarajan, M., Ambika, S., & Bharathi, K. (2015). Plant-extract mediated synthesis of ZnO nanoparticles using *Pongamia pinnata* and their activity against pathogenic bacteria. *Advanced powder technology*, 26(5), 1294-1299.
22. Fu, L., & Fu, Z. (2015). *Plectranthus amboinicus* leaf extract–assisted biosynthesis of ZnO nanoparticles and their photocatalytic activity. *Ceramics International*, 41(2), 2492-2496.
23. Stan, M., Popa, A., Toloman, D., Dehelean, A., Lung, I., & Katona, G. (2015). Enhanced photocatalytic degradation properties of zinc oxide nanoparticles synthesized by using plant extracts. *Materials Science in Semiconductor Processing*, 39, 23-29.
24. Grimley, D. A., & Oches, E. A. (2015). Amino acid geochronology of gastropod-bearing Pleistocene units in Illinois, central USA. *Quaternary Geochronology*, 25, 10-25.
25. Diallo, A., Beye, A. C., Doyle, T. B., Park, E., & Maaza, M. (2015). Green synthesis of Co₃O₄ nanoparticles via *Aspalathus linearis*: physical properties. *Green Chemistry Letters and Reviews*, 8(3-4), 30-36.
26. Sagar Raut, D. P., & Thorat, R. T. (2015). Green synthesis of zinc oxide (ZnO) nanoparticles using *Ocimum Tenuiflorum* leaves. *Int. J. Sci. Res*, 4, 1225-1228.
27. Suresh, D., Shobharani, R. M., Nethravathi, P. C., Kumar, M. P., Nagabhushana, H., & Sharma, S. C. (2015). *Artocarpus gomezianus* aided green synthesis of ZnO nanoparticles: Luminescence, photocatalytic and antioxidant properties. *Spectrochimica Acta Part A: Molecular and Biomolecular Spectroscopy*, 141, 128-134.
28. Suresh, D., Nethravathi, P. C., Rajanaika, H., Nagabhushana, H., & Sharma, S. C. (2015). Green synthesis of multifunctional zinc oxide (ZnO) nanoparticles using

- Cassia fistula plant extract and their photodegradative, antioxidant and antibacterial activities. *Materials Science in Semiconductor Processing*, 31, 446-454.
29. Hassan, S. S., El Azab, W. I., Ali, H. R., & Mansour, M. S. (2015). Green synthesis and characterization of ZnO nanoparticles for photocatalytic degradation of anthracene. *Advances in Natural Sciences: Nanoscience and Nanotechnology*, 6(4), 045012.
30. Janaki, A. C., Sailatha, E., & Gunasekaran, S. (2015). Synthesis, characteristics and antimicrobial activity of ZnO nanoparticles. *Spectrochimica Acta Part A: Molecular and Biomolecular Spectroscopy*, 144, 17-22.
31. Laokuldilok, N., Kopermsub, P., Thakeow, P., & Utama-ang, N. (2015). Microwave assisted extraction of bioactive compounds from turmeric (*Curcuma longa*). *International Journal of Agricultural Technology*, 11(5), 1185-1196
32. Sutradhar, P., & Saha, M. (2015). Synthesis of zinc oxide nanoparticles using tea leaf extract and its application for solar cell. *Bulletin of Materials Science*, 38, 653-657.
33. Elumalai, K., Velmurugan, S., Ravi, S., Kathiravan, V., & Ashokkumar, S. (2015). RETRACTED: Green synthesis of zinc oxide nanoparticles using *Moringa oleifera* leaf extract and evaluation of its antimicrobial activity.
34. Noorjahan, C. M., Shahina, S. J., Deepika, T., & Rafiq, S. (2015). Green synthesis and characterization of zinc oxide nanoparticles from Neem (*Azadirachta indica*). *International Journal of Scientific Engineering and Technology Research*, 4(30), 5751-5753.
35. Prabhu, Y. T., Rao, K. V., Kumari, B. S., Kumar, V. S. S., & Pavani, T. (2015). Synthesis of Fe₃O₄ nanoparticles and its antibacterial application. *International Nano Letters*, 5, 85-92.
36. Jagtap, P. K., Ratha, U., & Bhanjadeo, S. Eco compatible method for Synthesis of Zinc oxide Nanoparticle and Its Potential Applications.
37. Umaralikhan, L., & Jaffar, M. J. M. (2016). Green synthesis of ZnO and Mg doped ZnO nanoparticles, and its optical properties. *Journal of Materials Science: Materials in Electronics*, 28, 7677-7685.

38. Koupaei, M. H., Shareghi, B., Saboury, A. A., Davar, F., Semnani, A., & Evini, M. (2016). Green synthesis of zinc oxide nanoparticles and their effect on the stability and activity of proteinase K. *RSC advances*, 6(48), 42313-42323.
39. Fatimah, I. (2016). Green synthesis of silver nanoparticles using extract of *Parkia speciosa* Hassk pods assisted by microwave irradiation. *Journal of advanced research*, 7(6), 961-969.
40. Karnan, T., & Selvakumar, S. A. S. (2016). Biosynthesis of ZnO nanoparticles using rambutan (*Nephelium lappaceum*L.) peel extract and their photocatalytic activity on methyl orange dye. *Journal of molecular Structure*, 1125, 358-365.
41. Miller, V., Yusuf, S., Chow, C. K., Dehghan, M., Corsi, D. J., Lock, K., ... & Mente, A. (2016). Availability, affordability, and consumption of fruits and vegetables in 18 countries across income levels: findings from the Prospective Urban Rural Epidemiology (PURE) study. *The lancet global health*, 4(10), e695-e703.
42. Momeni, S. S., Nasrollahzadeh, M., & Rustaiyan, A. (2016). Green synthesis of the Cu/ZnO nanoparticles mediated by *Euphorbia prolifera* leaf extract and investigation of their catalytic activity. *Journal of colloid and interface science*, 472, 173-179.
43. Jyoti, K., Baunthiyal, M., & Singh, A. (2016). Characterization of silver nanoparticles synthesized using *Urtica dioica* Linn. leaves and their synergistic effects with antibiotics. *Journal of Radiation Research and Applied Sciences*, 9(3), 217-227.
44. Alalwan, A. A., Dwivedi, Y. K., Rana, N. P., & Williams, M. D. (2016). Consumer adoption of mobile banking in Jordan: Examining the role of usefulness, ease of use, perceived risk and self-efficacy. *Journal of Enterprise Information Management*, 29(1), 118-139.
45. Shabestarian, H., Homayouni-Tabrizi, M., Soltani, M., Namvar, F., Azizi, S., Mohamad, R., & Shabestarian, H. (2016). Green synthesis of gold nanoparticles using sumac aqueous extract and their antioxidant activity. *Materials Research*, 20, 264-270.

46. Rajan, A., Cherian, E., & Baskar, G. (2016). Biosynthesis of zinc oxide nanoparticles using *Aspergillus fumigatus* JCF and its antibacterial activity. *Int. J. Mod. Sci. Technol*, 1(2), 52-57.
47. Jafarirad, S., Mehrabi, M., Divband, B., & Kosari-Nasab, M. (2016). Biofabrication of zinc oxide nanoparticles using fruit extract of *Rosa canina* and their toxic potential against bacteria: A mechanistic approach. *Materials Science and Engineering: C*, 59, 296-302.
48. Shabestarian, H., Homayouni-Tabrizi, M., Soltani, M., Namvar, F., Azizi, S., Mohamad, R., & Shabestarian, H. (2016). Green synthesis of gold nanoparticles using sumac aqueous extract and their antioxidant activity. *Materials Research*, 20, 264-270.
49. Fowsiya, J., Madhumitha, G., Al-Dhabi, N. A., & Arasu, M. V. (2016). Photocatalytic degradation of Congo red using *Carissa edulis* extract capped zinc oxide nanoparticles. *Journal of Photochemistry and Photobiology B: Biology*, 162, 395-401.
50. Supraja, N., Prasad, T. N. V. K. V., Krishna, T. G., & David, E. (2016). Synthesis, characterization, and evaluation of the antimicrobial efficacy of *Boswellia ovalifoliolata* stem bark-extract-mediated zinc oxide nanoparticles. *Applied Nanoscience*, 6, 581-590.
51. Saranya, S., Vijayarani, K., & Pavithra, S. (2017). Green synthesis of iron nanoparticles using aqueous extract of *Musa ornata* flower sheath against pathogenic bacteria. *Indian Journal of Pharmaceutical Sciences*, 79(5), 688-694.
52. Gawade, V. V., Gavade, N. L., Shinde, H. M., Babar, S. B., Kadam, A. N., & Garadkar, K. M. (2017). Green synthesis of ZnO nanoparticles by using *Calotropis procera* leaves for the photodegradation of methyl orange. *Journal of Materials Science: Materials in Electronics*, 28, 14033-14039.
53. Rathnasamy, R., Thangasamy, P., Thangamuthu, R., Sampath, S., & Alagan, V. (2017). Green synthesis of ZnO nanoparticles using *Carica papaya* leaf extracts for photocatalytic and photovoltaic applications. *Journal of Materials Science: Materials in Electronics*, 28, 10374-10381.

54. Köerich, J. S., Nogueira, D. J., Vaz, V. P., Simioni, C., Silva, M. L. N. D., Ouriques, L. C., ... & Matias, W. G. (2020). Toxicity of binary mixtures of Al₂O₃ and ZnO nanoparticles toward fibroblast and bronchial epithelium cells. *Journal of toxicology and environmental health, part A*, 83(9), 363-377.
55. Lingaraju, K., Raja Naika, H., Manjunath, K., Basavaraj, R. B., Nagabhushana, H., Nagaraju, G., & Suresh, D. (2017). Biogenic synthesis of zinc oxide nanoparticles using *Ruta graveolens* (L.) and their antibacterial and antioxidant activities. *Applied Nanoscience*, 6, 703-710.
56. Karthik, S., Siva, P., Balu, K. S., Suriyaprabha, R., Rajendran, V., & Maaza, M. (2017). *Acalypha indica*-mediated green synthesis of ZnO nanostructures under differential thermal treatment: Effect on textile coating, hydrophobicity, UV resistance, and antibacterial activity. *Advanced Powder Technology*, 28(12), 3184-3194.
57. Vidya, C., Manjunatha, C., Chandraprabha, M. N., Rajshekar, M., & MAL, A. R. (2017). Hazard free green synthesis of ZnO nano-photo-catalyst using *Artocarpus Heterophyllus* leaf extract for the degradation of Congo red dye in water treatment applications. *Journal of environmental chemical engineering*, 5(4), 3172-3180.
58. Archana, B., Manjunath, K., Nagaraju, G., Sekhar, K. C., & Kottam, N. (2017). Enhanced photocatalytic hydrogen generation and photostability of ZnO nanoparticles obtained via green synthesis. *International Journal of Hydrogen Energy*, 42(8), 5125-5131.
59. Taghavi Fardood, S., Ramazani, A., Moradi, S., & Azimzadeh Asiabi, P. (2017). Green synthesis of zinc oxide nanoparticles using arabic gum and photocatalytic degradation of direct blue 129 dye under visible light. *Journal of Materials Science: Materials in Electronics*, 28, 13596-13601.
60. Siripireddy, B., & Mandal, B. K. (2017). Facile green synthesis of zinc oxide nanoparticles by *Eucalyptus globulus* and their photocatalytic and antioxidant activity. *Advanced Powder Technology*, 28(3), 785-797.
61. Nava, O. J., Soto-Robles, C. A., Gómez-Gutiérrez, C. M., Vilchis-Nestor, A. R., Castro-Beltrán, A., Olivas, A., & Luque, P. A. (2017). Fruit peel extract mediated

- green synthesis of zinc oxide nanoparticles. *Journal of Molecular Structure*, 1147, 1-6.
62. Nava, O. J., Luque, P. A., Gómez-Gutiérrez, C. M., Vilchis-Nestor, A. R., Castro-Beltrán, A., Mota-González, M. L., & Olivas, A. (2017). Influence of *Camellia sinensis* extract on Zinc Oxide nanoparticle green synthesis. *Journal of Molecular Structure*, 1134, 121-125.
63. Rajaboopathi, S., & Thambidurai, S. (2017). *Green synthesis of seaweed surfactant based CdO-ZnO nanoparticles for better thermal and photocatalytic activity. Current Applied Physics*, 17(12), 1622–1638. doi:10.1016/j.cap.2017.09.006
64. Furhan, & Ramesan, M. T. (2022). Zinc oxide reinforced poly (para-aminophenol) nanocomposites: Structural, thermal stability, conductivity and ammonia gas sensing applications. *Journal of Macromolecular Science, Part A*, 59(10), 675-688.
65. Bhuvaneshwari, S., Subashini, G., & Subramaniam, S. (2017). Green synthesis of zinc oxide nanoparticles using potato peel and degradation of textile mill effluent by photocatalytic activity. *World J. Pharm. Res*, 6, 774-785.
66. Chaudhuri, S. K., & Malodia, L. (2017). Biosynthesis of zinc oxide nanoparticles using leaf extract of *Calotropis gigantea*: characterization and its evaluation on tree seedling growth in nursery stage. *Applied Nanoscience*, 7(8), 501-512.
67. Paul, B., Vadivel, S., Dhar, S. S., Debbarma, S., & Kumaravel, M. (2017). One-pot green synthesis of zinc oxide nano rice and its application as sonocatalyst for degradation of organic dye and synthesis of 2-benzimidazole derivatives. *Journal of Physics and Chemistry of Solids*, 104, 152-159.
68. Agarwal, H., Kumar, S. V., & Rajeshkumar, S. (2017). A review on green synthesis of zinc oxide nanoparticles—An eco-friendly approach. *Resource-Efficient Technologies*, 3(4), 406-413.
69. Khalil, A. T., Ovais, M., Ullah, I., Ali, M., Shinwari, Z. K., Khamlich, S., & Maaza, M. (2017). *Sageretia thea* (Osbeck.) mediated synthesis of zinc oxide nanoparticles and its biological applications. *Nanomedicine*, 12(15), 1767-1789.
70. Boroumand Moghaddam, A., Moniri, M., Azizi, S., Abdul Rahim, R., Bin Ariff, A., Navaderi, M., & Mohamad, R. (2017). Eco-friendly formulated zinc oxide

nanoparticles: induction of cell cycle arrest and apoptosis in the MCF-7 cancer cell line. *Genes*, 8(10), 281.

71. Rajendran, S. P., & Sengodan, K. (2017). Synthesis and characterization of zinc oxide and iron oxide nanoparticles using *Sesbania grandiflora* leaf extract as reducing agent. *Journal of Nanoscience*, 2017.
72. Kokabi, M., Yousefzadi, M., Nejad Ebrahimi, S., & Zarei, M. (2017). Green synthesis of zinc oxide nanoparticles using Seaweed aqueous extract and evaluation of antibacterial and ecotoxicological activity. *Journal of Nanoscience*, 8(6), 27(8).
73. Malaikozhundan, B., Vaseeharan, B., Vijayakumar, S., Pandiselvi, K., Kalanjiam, M. A. R., Murugan, K., & Benelli, G. (2017). Biological therapeutics of *Pongamia pinnata* coated zinc oxide nanoparticles against clinically important pathogenic bacteria, fungi and MCF-7 breast cancer cells. *Microbial pathogenesis*, 104, 268-277.
74. Rehana, D., Mahendiran, D., Kumar, R. S., & Rahiman, A. K. (2017). In vitro antioxidant and antidiabetic activities of zinc oxide nanoparticles synthesized using different plant extracts. *Bioprocess and biosystems engineering*, 40(6), 943-957.
75. Kavitha, S., Dhamodaran, M., Prasad, R., & Ganesan, M. (2017). Synthesis and characterisation of zinc oxide nanoparticles using terpenoid fractions of *Andrographis paniculata* leaves. *International Nano Letters*, 7, 141-147.
76. Khajuria, A. K., Bisht, N. S., & Kumar, G. (2017). Synthesis of Zinc oxide nanoparticles using leaf extract of *Viola canescens* Wall. ex, Roxb. and their antimicrobial activity. *Journal of Pharmacognosy and Phytochemistry*, 6(5), 1301-1304.
77. Jeyabharathi, S., Kalishwaralal, K., Sundar, K., & Muthukumaran, A. (2017). Synthesis of zinc oxide nanoparticles (ZnONPs) by aqueous extract of *Amaranthus caudatus* and evaluation of their toxicity and antimicrobial activity. *Materials Letters*, 209, 295-298.
78. Murali, M., Mahendra, C., Rajashekar, N., Sudarshana, M. S., Raveesha, K. A., & Amruthesh, K. N. (2017). Antibacterial and antioxidant properties of biosynthesized zinc oxide nanoparticles from *Ceropegia candelabrum* L.—an

endemic species. *Spectrochimica Acta Part A: Molecular and Biomolecular Spectroscopy*, 179, 104-109.

79. Manokari, M., & Shekhawat, M. S. (2017). Green synthesis of zinc oxide nanoparticles using whole plant extracts of *Cassia tora* L. and their characterization. *Journal of Scientific Achievements*, 2(8), 10-16.
80. Datta, A., Patra, C., Bharadwaj, H., Kaur, S., Dimri, N., & Khajuria, R. (2017). Green synthesis of zinc oxide nanoparticles using parthenium hysterophorus leaf extract and evaluation of their antibacterial properties. *J. Biotechnol. Biomater*, 7(3), 271-276.